Electronic Supplementary Material (ESI) for Dalton Transactions.

Supplementary Information

Nitratoethyl-5*H*-tetrazoles: Improving Oxygen Balance through Application of Organic Nitrates in Energetic Coordination Compounds

Michael S. Gruhne, Tobias Lenz, Markus Rösch, Marcus Lommel,

Maximilian H. H. Wurzenberger, Thomas M. Klapötke, and Jörg Stierstorfer*

[a] Department of Chemistry, Ludwig-Maximilian University of Munich,

Butenandtstr. 5-13, D-81377 Munich, Germany.

Dr. Jörg Stierstorfer, jstch@cup.uni-muenchen.de, FAX +49 89 2180 77007

Table of Contents

1. Compounds Overview

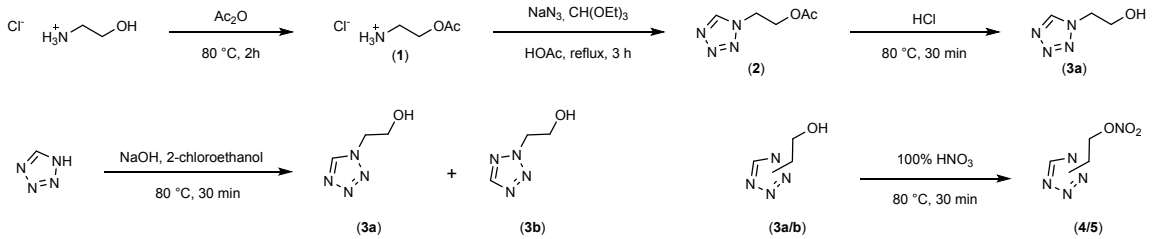

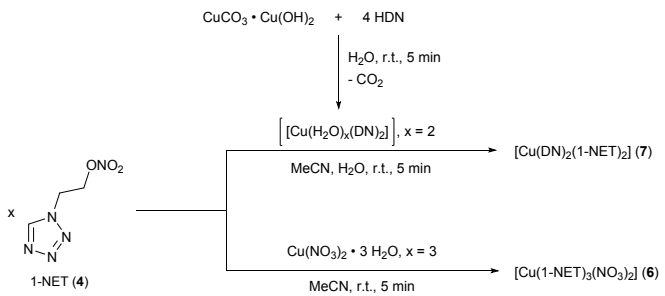

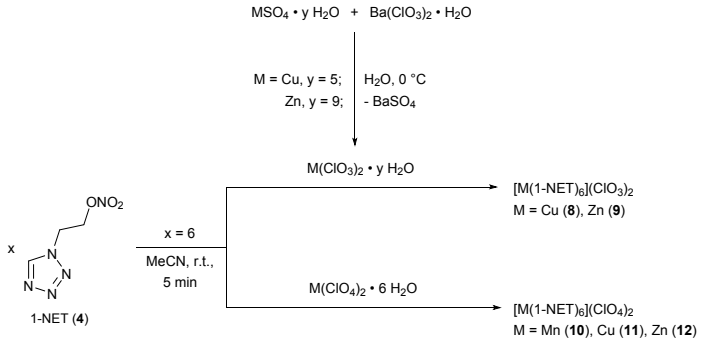

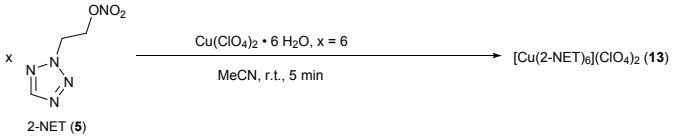

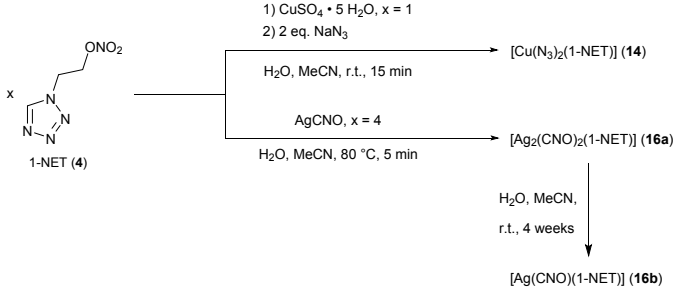

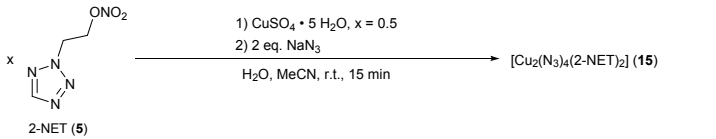

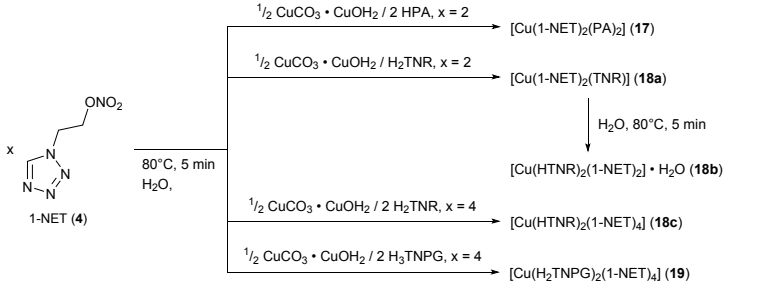

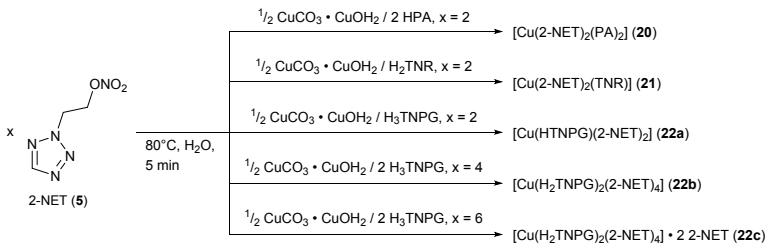

2. Single Crystal X-Ray Diffraction

For all crystalline compounds, an Oxford Xcalibur3 diffractometer with a CCD area detector or Bruker D8 Venture TXS diffractometer equipped with a multilayer monochromator, a Photon 2 detector and a rotating-anode generator were employed for data collection using Mo-K_α radiation (λ = 0.7107 Å). On the Oxford device, data collection and reduction were carried out using the CrysAlisPRO software.[S1] On the Bruker diffractometer, the data were collected with the Bruker Instrument Service v3.0.21, the data reduction was performed using the SAINT V8.18C software (Bruker AXS Inc., 2011). The structures were solved by direct methods (SIR-92,[S2] SIR-97,[S3,S4] SHELXS-97[S5,S6] or SHELXT[S7]) and refined by full-matrix least-squares on *F*2 (SHELXL[S5,S6]) and finally checked using the PLATON software[S8] integrated in the WinGX[S7] or Olex2[S8] software suite. The non-hydrogen atoms were refined anisotropically and the hydrogen atoms were located and freely refined. The absorptions were corrected by a SCALE3 ABSPACK or SADABS Bruker APEX3 multi-scan method.[S11,S12] All DIAMOND2 plots are shown with thermal ellipsoids at the 50% probability level and hydrogen atoms are shown as small spheres of arbitrary radius.

Table S1. Crystallographic data of **2**, **4**, and **5**.

	2	**4**	**5**
Formula	$C_5H_8N_4O_2$	$C_3H_5N_5O_3$	$C_3H_5N_5O_3$
FW (g mol^{-1})	156.15	159.12	159.12
Crystal system	monoclinic	monoclinic	orthorhombic
Space Group	$P2_1/c$	$P2_1/c$	$Pna2_1$
Color / Habit	colorless block	colorless block	colorless needle
Size (mm)	0.31 x 0.50 x 0.50	0.32 x 0.50 x 0.50	0.24 x 0.33 x 0.50
a (Å)	7.6852(9)	20.8315(6)	7.3292(8)
b (Å)	14.3722(13)	6.5682(2)	14.3427(15)
c (Å)	6.6944(6)	9.8140(3)	6.3485(5)
α (°)	90	90	90
β (°)	104.152(10)	103.473(3)	90
γ (°)	90	90	90
V (Å^3)	716.98(13)	1305.85(7)	667.36(11)
Z	4	8	4
$\rho_{calc.}$ (g cm^{-3})	1.447	1.619	1.584
μ (mm^{-1})	0.115	0.143	0.140
F(000)	328	656	328
$\lambda_{MoK\alpha}$ (Å)	0.71073	0.71073	0.71073
T (K)	106	105	128
θ Min–Max (°)	2.7, 26.4	3.3, 26.4	2.8, 26.4
Dataset	−5:9; −10:17; −8:6	−26:26; −8:8; −12:12	−9:9; −17:17; −7:7
Reflections collected	3119	28160	9133
Independent refl.	1466	2669	1355
R_{int}	0.022	0.030	0.048
Observed reflections	1165	2378	1160
Parameters	132	199	120
R_1 (obs)[a]	0.0352	0.0339	0.0361
wR_2 (all data)[b]	0.0830	0.0793	0.0806
GooF[c]	1.07	1.12	1.06
Resd. Dens. (e Å^{-3})	−0.22, 0.17	−0.17, 0.19	−0.17, 0.19
Absorption correction	multi-scan	multi-scan	multi-scan
Device type	Oxford Xcalibur3	Oxford Xcalibur3	Oxford Xcalibur3
CCDC	2080666	2080674	2080685

[a] $R_1 = \Sigma||F_0|-|F_c||/\Sigma|F_0|$; [b] $wR_2 = [\Sigma[w(F_0^2-F_c^2)^2]/\Sigma[w(F_0)^2]]^{1/2}$; $w = [\sigma c^2(F_0^2)+(xP)^2+yP]^{-1}$ and $P = (F_0^2+2F_c^2)/3$; c) GooF = $\{\Sigma[w(F_o^2-F_c^2)^2]/(n-p)\}^{1/2}$ (n = number of reflections; p = total number of parameters).

Table S2. Crystallographic data of **6**–**8**.

	6	**7**	**8**
Formula	$C_9H_{15}CuN_{17}O_{15}$	$C_6H_{10}CuN_{16}O_{14}$	$C_{18}H_{30}Cl_2CuN_{30}O_{24}$
FW (g mol^{-1})	664.92	593.84	1185.16
Crystal system	monoclinic	monoclinic	monoclinic
Space Group	$P2_1/c$	$P2_1/c$	Cc
Color / Habit	blue plate	blue plate	blue platelet
Size (mm)	0.08 x 0.38 x 0.50	0.04 x 0.37 x 0.59	0.05 x 0.08 x 0.09
a (Å)	20.6706(13)	13.1234(9)	10.721(3)
b (Å)	7.2984(4)	6.3864(5)	18.897(5)
c (Å)	16.4791(9)	12.8363(8)	23.186(6)
α (°)	90	90	90
β (°)	109.752(7)	110.160(6)	97.284(10)
γ (°)	90	90	90
V (Å^3)	2339.8(3)	1009.92(13)	4660(2)
Z	4	2	4
$\rho_{calc.}$ (g cm^{-3})	1.888	1.953	1.689
μ (mm^{-1})	1.045	1.193	0.698
F(000)	1348	598	2412
$\lambda_{MoK\alpha}$ (Å)	0.71073	0.71073	0.71073
T (K)	99	102	100
θ Min–Max (°)	2.5, 26.4	3.2, 26.4	2.2, 26.4
Dataset	−25: 25; −9: 9; −20: 19	−16: 16; −7: 7; −15: 16	−13: 13; −23: 23; −28: 28
Reflections collected	14785	6571	33018
Independent refl.	4786	2048	8963
R_{int}	0.056	0.030	0.058
Observed reflections	3516	1748	7792
Parameters	379	169	659
R_1 (obs)[a]	0.0442	0.0290	0.0646
wR_2 (all data)[b]	0.0916	0.0743	0.1824
GooF[c]	1.02	1.08	1.04
Resd. Dens. (e Å^{-3})	−0.59, 0.57	−0.26, 0.39	−1.04, 0.85
Absorption correction	multi-scan	multi-scan	multi-scan
Device type	Oxford Xcalibur3	Oxford Xcalibur3	Bruker D8 Venture TXS
CCDC	2080679	2080675	2080677

[a] $R_1 = \Sigma||F_0|-|F_c||/\Sigma|F_0|$; [b] $wR_2 = [\Sigma[w(F_0^2-F_c^2)^2]/\Sigma[w(F_0)^2]]^{1/2}$; $w = [\sigma c^2(F_0^2)+(xP)^2+yP]^{-1}$ and $P = (F_0^2+2F_c^2)/3$; c) GooF = $\{\Sigma[w(F_o^2-F_c^2)^2]/(n-p)\}^{1/2}$ (n = number of reflections; p = total number of parameters).

Table S3. Crystallographic data of **10**, **11**, **12**, and **14**.

	10	**11**	**12**	**14**
Formula	$C_{18}H_{30}Cl_2MnN_{30}O_{26}$	$C_{18}H_{30}Cl_2CuN_{30}O_{26}$	$C_{18}H_{30}Cl_2N_{30}O_{26}Zn$	$C_6H_{10}Cu_2N_{22}O_6$
FW (g mol^{-1})	1208.56	1217.16	1218.99	613.44
Crystal system	triclinic	triclinic	triclinic	triclinic
Space Group	*P*–1	*P*–1	*P*–1	*P*-1
Color / Habit	colorless block	blue block	colorless block	brown platelet
Size (mm)	0.11 x 0.18 x 0.47	0.20 x 0.48 x 0.50	0.21 x 0.39 x 0.50	0.01 x 0.03 x 0.03
a (Å)	10.9319(8)	10.8193(9)	10.8769(8)	6.2622(4)
b (Å)	10.9517(6)	10.9055(10)	10.8942(9)	10.5985(8)
c (Å)	12.4811(7)	12.2584(10)	12.4267(12)	15.9381(14)
α (°)	88.318(4)	88.625(7)	68.548(8)	102.119(3)
β (°)	68.294(6)	68.707(8)	88.553(7)	96.226(3)
γ (°)	61.051(7)	61.944(9)	61.016(8)	91.774(3)
V (Å^3)	1194.09(17)	1170.2(2)	1177.8(2)	1026.56(14)
Z	1	1	1	2
$\rho_{calc.}$ (g cm^{-3})	1.681	1.727	1.719	1.985
μ (mm^{-1})	0.505	0.700	0.754	2.155
F(000)	615	619	620	612
$\lambda_{MoK\alpha}$ (Å)	0.71073	0.71073	0.71073	0.71073
T (K)	123	114	102	173
θ Min–Max (°)	2.5, 26.4	2.3, 26.4	2.2, 26.4	2.0, 26.4
Dataset	−13: 13; −13: 13; −15: 15	−13:13; −11:13; −15:15	−13:13; −13:12; −15:14	−7: 7; −13: 13; −19: 19
Reflections collected	18055	7824	9471	11434
Independent refl.	4868	4720	4809	4172
R_{int}	0.054	0.037	0.039	0.040
Observed reflections	3535	3314	3302	3184
Parameters	349	349	349	325
R_1 (obs)[a]	0.0452	0.0538	0.0513	0.0397
wR_2 (all data)[b]	0.1146	0.1041	0.1045	0.0789
GooF[c]	1.04	1.03	1.04	1.05
Resd. Dens. (e Å^{-3})	−0.31, 0.58	−0.46, 0.63	–0.45, 0.56	−0.38, 0.39
Absorption correction	multi-scan	multi-scan	multi-scan	multi-scan
Device type	Oxford Xcalibur3	Oxford Xcalibur3	Oxford Xcalibur3	Bruker D8 Venture TXS
CCDC	2080672	2080669	2080683	2080678

[a] $R_1 = \Sigma||F_0|-|F_c||/\Sigma|F_0|$; [b] $wR_2 = [\Sigma[w(F_0^2-F_c^2)^2]/\Sigma[w(F_0)^2]]^{1/2}$; $w = [\sigma c^2(F_0^2)+(xP)^2+yP]^{-1}$ and $P = (F_0^2+2F_c^2)/3$; c) GooF = $\{\Sigma[w(F_o^2-F_c^2)^2]/(n-p)\}^{1/2}$ (n = number of reflections; p = total number of parameters).

Table S4. Crystallographic data of **15**, **16a**, **16b**, and **17**.

	15	**16a**	**16b**	**17**
Formula	$C_3H_5Cu_2N_{17}O_3$	$C_5H_5Ag_2N_7O_5$	$C_4H_5AgN_6O_4$	$C_{18}H_{14}CuN_{16}O_{20}$
FW (g mol^{-1})	454.32	458.90	309.01	837.99
Crystal system	monoclinic	monoclinic	monoclinic	monoclinic
Space Group	$P2_1/n$	$I2/a$	$P2_1/c$	$P2_1/c$
Color / Habit	brown platelet	colorless platelet	colorless platelet	green platelet
Size (mm)	0.01 x 0.25 x 0.25	0.09 x 0.25 x 0.50	0.02 x 0.07 x 0.10	0.02 x 0.05 x 0.05
a (Å)	15.7453(11)	12.5931(10)	15.0209(6)	8.0432(4)
b (Å)	5.7379(4)	5.6798(3)	5.4770(2)	17.7448(8)
c (Å)	16.3858(14)	31.354(3)	10.6783(5)	21.2063(11)
α (°)	90	90	90	90
β (°)	109.892(9)	90.669(7)	91.237(2)	96.689(2)
γ (°)	90	90	90	90
V (Å^3)	1392.1(2)	2242.5(3)	878.29(6)	3006.1(3)
Z	4	8	4	4
$\rho_{calc.}$ (g cm^{-3})	2.168	2.718	2.337	1.852
μ (mm^{-1})	3.111	3.525	2.303	0.846
F(000)	896	1744	600	1692
$\lambda_{MoK\alpha}$ (Å)	0.71073	0.71073	0.71073	0.71073
T (K)	123	104	173	173
θ Min–Max (°)	2.2, 26.4	2.6, 26.4	4.0, 26.4	2.3, 26.4
Dataset	−19: 19; −5: 7; −20: 20	−15: 15; −7: 6; −38: 39	−18: 18; −6: 6; −13: 12	−10: 10; −22: 22; −26: 26
Reflections collected	9140	8676	12974	55744
Independent refl.	2839	2296	1764	6146
R_{int}	0.067	0.030	0.033	0.054
Observed reflections	1971	1864	1672	5073
Parameters	226	172	136	525
R_1 (obs)[a]	0.0514	0.0251	0.0181	0.0390
wR_2 (all data)[b]	0.1124	0.0616	0.0423	0.0979
GooF[c]	1.02	1.04	1.06	1.07
Resd. Dens. (e Å^{-3})	−0.63, 0.75	−0.51, 0.92	−0.65, 0.93	−0.41, 0.56
Absorption correction	multi-scan	multi-scan	multi-scan	multi-scan
Device type	Oxford Xcalibur3	Oxford Xcalibur3	Bruker D8 Venture TXS	Bruker D8 Venture TXS
CCDC	2080684	2080673	2080682	2080680

[a] $R_1 = \Sigma||F_0|-|F_c||/\Sigma|F_0|$; [b] $wR_2 = [\Sigma[w(F_0^2-F_c^2)^2]/\Sigma[w(F_0)^2]]^{1/2}$; $w = [\sigma c^2(F_0^2)+(xP)^2+yP]^{-1}$ and $P = (F_0^2+2F_c^2)/3$; c) GooF = $\{\Sigma[w(F_o^2-F_c^2)^2]/(n-p)\}^{1/2}$ (n = number of reflections; p = total number of parameters).

Table S5. Crystallographic data of **18b**, **18c**, **19**, and **20**.

	18b	**18c**	**19**	**20**
Formula	$C_{18}H_{16}CuN_{16}O_{23}$	$C_{24}H_{24}CuN_{26}O_{28}$	$C_{24}H_{24}CuN_{26}O_{30}$	$C_{18}H_{14}CuN_{16}O_{20}$
FW (g mol^{-1})	888.01	1188.23	1220.23	837.99
Crystal system	monoclinic	triclinic	triclinic	triclinic
Space Group	$P2_1/c$	$P\bar{1}$	$P\bar{1}$	$P\bar{1}$
Color / Habit	green block	green block	green plate	green block
Size (mm)	0.05 x 0.09 x 0.13	0.08 x 0.19 x 0.47	0.05 x 0.25 x 0.50	0.12 x 0.29 x 0.48
a (Å)	14.2845(14)	8.9977(6)	9.0040(7)	6.5499(4)
b (Å)	22.033(2)	10.9877(7)	10.8642(9)	8.7690(6)
c (Å)	10.1252(9)	12.9353(9)	12.9713(12)	14.0403(11)
α (°)	90	88.113(5)	87.922(7)	71.967(6)
β (°)	99.740(4)	69.868(7)	69.740(8)	89.224(5)
γ (°)	90	66.507(7)	67.742(8)	74.396(5)
V (Å^3)	3140.8(5)	1093.07(15)	1095.07(19)	736.40(10)
Z	4	1	1	1
$\rho_{calc.}$ (g cm^{-3})	1.878	1.805	1.850	1.890
μ (mm^{-1})	0.822	0.630	0.635	0.864
F(000)	1796	603	619	423
$\lambda_{MoK\alpha}$ (Å)	0.71073	0.71073	0.71073	0.71073
T (K)	173	101	100	132
θ Min–Max (°)	2.2, 27.5	2.0, 26.4	2.0, 26.4	2.5, 26.4
Dataset	−18: 18; −28: 28; −12: 13	−10: 11; −13: 13; −16: 16	−11: 10; −13: 12; −16: 13	−7: 8; −10: 10; −17: 17
Reflections collected	55212	7022	7691	5569
Independent refl.	7225	4407	4462	3006
R_{int}	0.047	0.025	0.054	0.028
Observed reflections	6349	3673	2743	2432
Parameters	548	435	427	250
R_1 (obs)[a]	0.0597	0.0429	0.0636	0.0432
wR_2 (all data)[b]	0.1752	0.1062	0.1326	0.0949
GooF[c]	1.04	1.03	1.03	1.03
Resd. Dens. (e Å^{-3})	−0.83, 2.36	−0.46, 0.42	−0.57, 0.65	−0.56, 0.48
Absorption correction	multi-scan	multi-scan	multi-scan	multi-scan
Device type	Bruker D8 Venture TXS	Oxford Xcalibur3	Oxford Xcalibur3	Oxford Xcalibur3
CCDC		2080676	2080681	2080671

[a] $R_1 = \Sigma||F_0|-|F_c||/\Sigma|F_0|$; [b] $wR_2 = [\Sigma[w(F_0^2-F_c^2)^2]/\Sigma[w(F_0)^2]]^{1/2}$; $w = [\sigma c^2(F_0^2)+(xP)^2+yP]^{-1}$ and $P = (F_0^2+2F_c^2)/3$; c) GooF = $\{\Sigma[w(F_o^2-F_c^2)^2]/(n-p)\}^{1/2}$ (n = number of reflections; p = total number of parameters).

Table S6. Crystallographic data of **21**, **22a**, and **22c**.

	21	**22a**	**22c**
Formula	$C_{12}H_{11}CuN_{13}O_{14}$	$C_{12}H_{11}CuN_{13}O_{15}$	$C_{30}H_{34}CuN_{36}O_{36}$
FW (g mol^{-1})	624.88	640.88	1538.48
Crystal system	triclinic	triclinic	triclinic
Space Group	*P*–1	*P*–1	*P*–1
Color / Habit	green plate	dark green block	green platelet
Size (mm)	0.11 x 0.25 x 0.54	0.14 x 0.20 x 0.34	0.06 x 0.30 x 0.38
a (Å)	10.1859(8)	10.3415(6)	8.4568(6)
b (Å)	10.4855(8)	10.4028(6)	11.2204(8)
c (Å)	10.8414(7)	10.8539(6)	16.7588(10)
α (°)	72.332(6)	71.766(5)	101.080(5)
β (°)	77.521(6)	78.429(5)	103.168(5)
γ (°)	81.225(6)	80.742(5)	107.579(6)
V (Å^3)	1072.51(14)	1080.44(11)	1416.56(19)
Z	2	2	1
$\rho_{calc.}$ (g cm^{-3})	1.935	1.970	1.804
μ (mm^{-1})	1.125	1.123	0.524
F(000)	630	646	783
$\lambda_{MoK\alpha}$ (Å)	0.71073	0.71073	0.71073
T (K)	102	102	123
θ Min–Max (°)	2.0, 26.4	2.0, 26.4	2.0, 26.4
Dataset	−12:12; −13:13; −13:13	−12: 12; −12: 13; −12: 13	−10:10; −14:14; −20:20
Reflections collected	7539	8987	21342
Independent refl.	4401	4412	5794
R_{int}	0.032	0.028	0.087
Observed reflections	3331	3696	3757
Parameters	364	374	468
R_1 (obs)[a]	0.0486	0.0348	0.0534
wR_2 (all data)[b]	0.1363	0.0880	0.1184
GooF[c]	1.06	1.03	1.02
Resd. Dens. (e Å^{-3})	−0.59, 0.58	−0.37, 0.46	−0.48, 0.72
Absorption correction	multi-scan	multi-scan	multi-scan
Device type	Oxford Xcalibur3	Oxford Xcalibur3	Oxford Xcalibur3
CCDC	2080667	2080670	2080668

[a] $R_1 = \Sigma||F_0|-|F_c||/\Sigma|F_0|$; [b] $wR_2 = [\Sigma[w(F_0^2-F_c^2)^2]/\Sigma[w(F_0)^2]]^{1/2}$; $w = [\sigma c^2(F_0^2)+(xP)^2+yP]^{-1}$ and $P = (F_0^2+2F_c^2)/3$; c) GooF = $\{\Sigma[w(F_o^2-F_c^2)^2]/(n-p)\}^{1/2}$ (n = number of reflections; p = total number of parameters).

The tetrazole derivative **2** crystallizes in the form of colorless blocks in the monoclinic space group $P2_1/c$, with four formula units per unit cell. The calculated density of 1.447 g cm^{-3} at 106 K is lower than the densities observed for the tetrazoles **4** and **5**. The methylene groups are, as already observed for the compounds **4** and **5**, arranged in a slighty distorted gauche conformation (N1–C2-C3–O1 = 69.01(12) °, Figure S1). The bond lengths and angles in the tetrazole moiety are similar to the ones observed in 1-NET (**4**) and 2-NET (**5**).

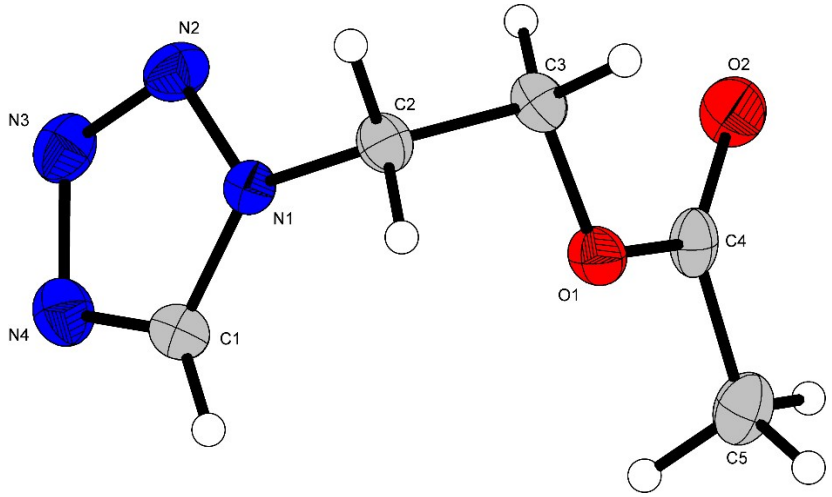

Figure S1. Molecular unit the tetrazole derivative **2**. Selected bond lengths (Å): N1-C2 1.4620(17), C2-C3 1.5018(19), C3–O1 1.4490(17), O1–C4 1.3448(16), O2–C4 1.2043(17), C4–C5 1.488(2). Selected bond angles (°): N1–C2–C3 111.11(11), C2–C3-O1 106.74(11), C3–O1–C4 116.47(10), O1–C4–O2 122.84(13), O1–C4–C5 110.96(13).

The manganese(II) and zinc(II) coordination compounds **10** and **12**, along with the copper(II) perchlorate complex **11**, crystallize isotypically in the triclinic space group *P*−1 with one formula unit per unit cell. As already stated for the copper complex, the compounds' densities differ only slightly, with compound **11** showing the highest value (**10**: 1.681 g cm^{-3} at 123 K; **11**: 1.727 g cm^{-3} at 114 K; **12**: 1.719 g cm^{-3}). Each perchlorate complex shows an octahedral coordination sphere (Figure S2) built up by six moieties of 1-NET (**4**).

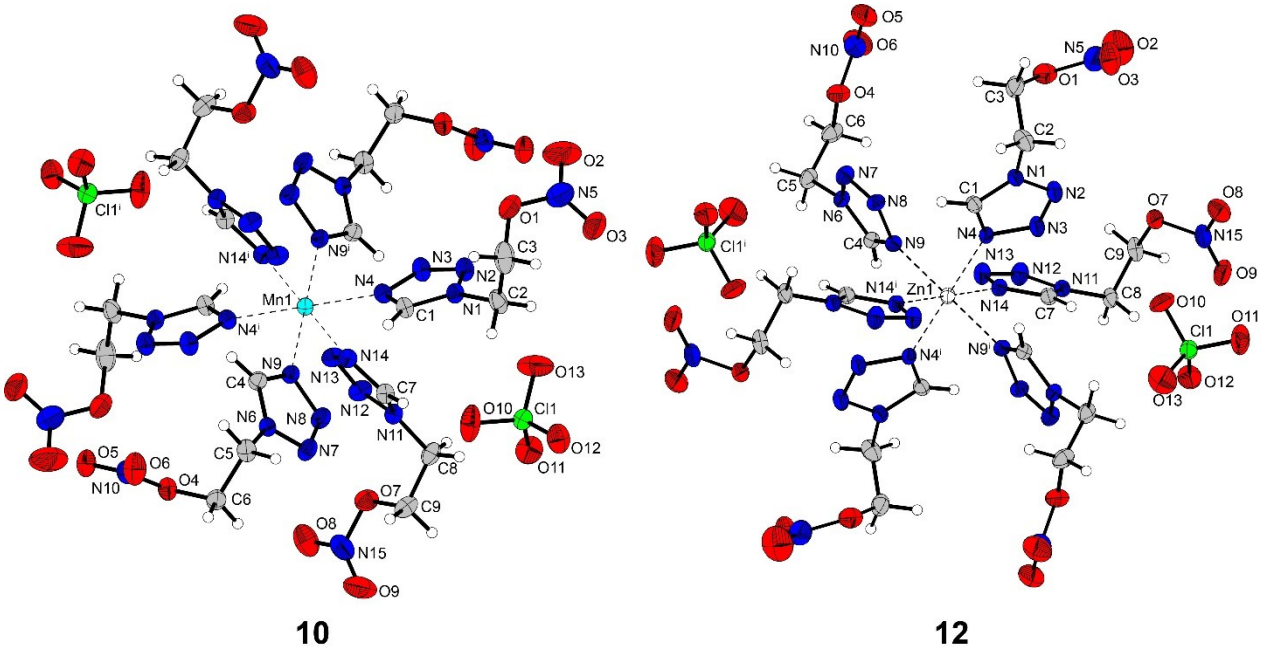

10 **12**

Figure S2. Molecular units of $[Mn(1\text{-}NET)_6](ClO_4)_2$ (**10**, left) and $[Zn(1\text{-}NET)_6](ClO_4)_2$ (**12**, right). Selected bond lengths (Å) of **10**: Mn1–N4 2.23171 (14), Mn–N9 (2.2482(3), Mn1–N14 2.24903(14). Selected bond lengths (Å) of **12**: Zn1–N4 2.143(3), Zn1–N9 2.154(3), Zn1–N14 2.170(2). Selected bond angles (°) of **10**: N9–Mn1–N14 91.803(7), N4–Mn1–N14 86.912(5), N4–Mn1–N9 89.510(7). Selected bond angles (°) of **12**: N4–Zn1–N9 92.10(13), N4–Zn1–N14 90.32(11), N9–Zn1–N14 91.67(11). Symmetry code of **10**: (i) 1−x, 1−y, 1−z. Symmetry code of **12**: (i) 1−x, 2−y, −z.

In contrast to compound **14**, the copper(II) azide complex **15** crystallizes in the triclinic space group *P*−1. The asymmetric unit in this case is made up of only one instead of two molecular units and contains two copper azide moieties per tetrazole unit (Figure S3, A). The unit cell is built up by four formula units, resulting in a higher density of 2.168 g cm^{-3} at 123 K. Every copper atom is coordinated octahedrally. While Cu2 is solely coordinated through azide moieties, the other cental metal (Cu1) is also complexed by a 2-NET ligand. Every anion is linking between two metal centers, whereas three different types of linking were observed (Figure S3, B). The frist mode, represented by the N9–N10–N11 anion, is solely linking Cu1 and Cu2. The N12–N13–N14 and the N15–N16–N17 azide moieties are forming the bonds all originating from the same nitrogen atom. Two of these bonds are within the same asymmetric unit. The third bond is within another asymmetric unit and therefore leading to the formation of 1D polymeric chains. The third coordination mode (N8–N7–N6) is also linking between three copper centers. The first two bonds are again between the same assymetric unit, the third bond is leading to the formation of 2D polymeric layers (Figure S3, C).

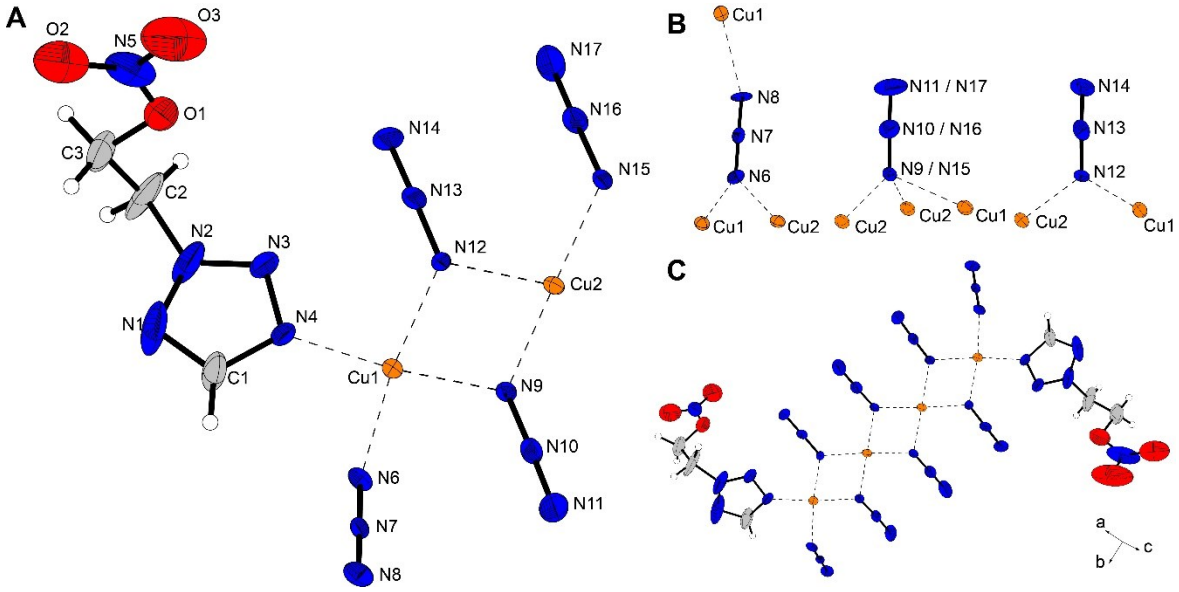

Figure S3. A: Molecular unit of complex **15**. Selected bond lengths (Å): Cu1–N4 1.97343(13), Cu1–N6 1.98651(10), Cu1–N9 2.02128(11), Cu1–N12 1.99045(13), Cu2–N9 1.99224(12), Cu2–N12 1.99898(11), Cu2–N15 2.00955(14). Selected bond angles (°): N9–Cu1–N12 77.168(5), N4–Cu1–N6 90.720(5), N9–Cu2–N12 77.643(5). **B**: Coordination modes of the azide anions in **15**. **C**: Section of the polymeric network formed by ECC **15**.

The copper(II) complex **18b**, based on the $HTNR^-$ anion crystallizes in the monoclinic space group $P2_1/c$ with four formula units per unit cell. The calculated densitiy of 1.878 g cm^{-3} at 173 K is only slightly higher than the one of **18c** based on the same anion (1.805 g cm^{-3} at 101 K). Like ECC **18c**,a octahedral coordination sphere is formed. However, the coordination sphere found in complex **18b** is built up by two ligand moieties, whereas in coordination compound **18c** four ligand units can be found (Figure S4). Futhermore, the anions and the ligands are arranged in *cis*-conformation and the formed octahedral is stongly distorted (O14-Cu1–O22 = 162.73(9) °). The complex is also the only observed coordination compound incooperating an aqua moiety together with NET ligands.

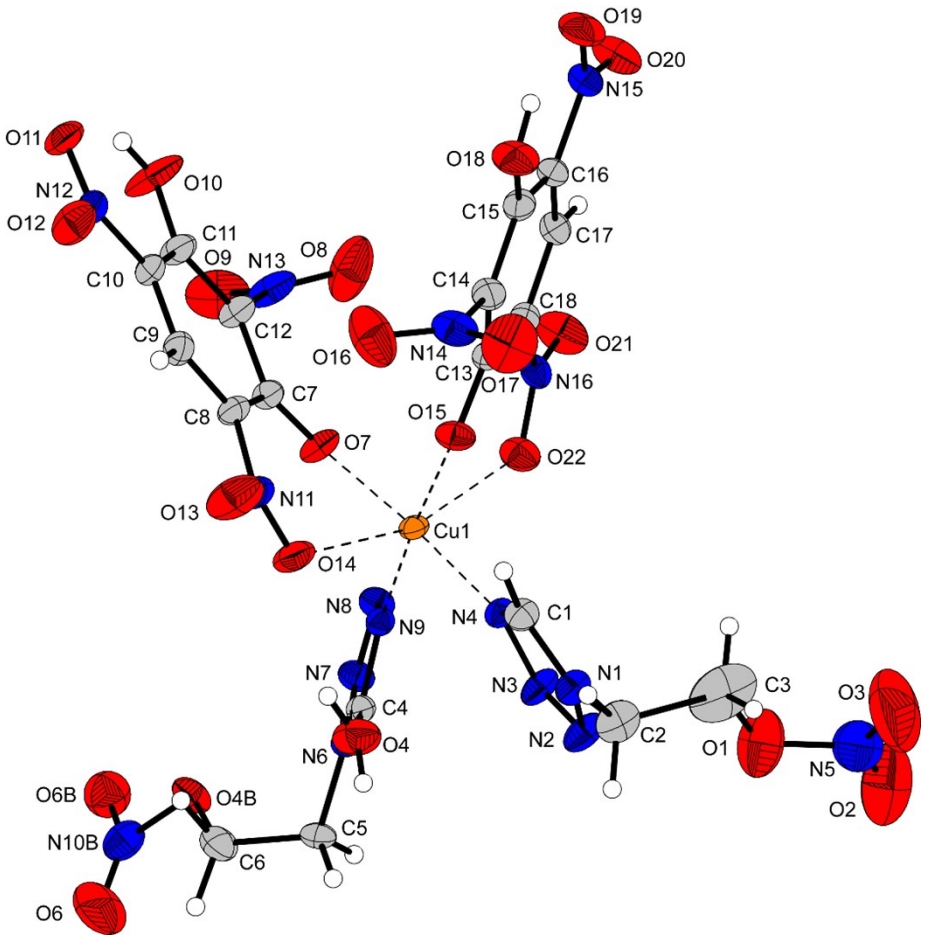

Figure S4. Molecular formula of $[Cu(HTNR)_2(1\text{-}NET)_2] \bullet H_2O$ (**18b**). Slelected bond lenghts (Å): Cu1–N4 2.001(3), Cu1–N9 1.991(3), Cu1–O7 1.950(3), Cu1–O15 1.951(2), Cu1–O14 2.349(3), Cu1–O22 2.306(3). Selected bond angles (°): O15–Cu1–N4 86.38(11), O15–Cu1–O7 91.54(10), O15-Cu1–O22 80.83(9).

The copper(II) complexes **18c** and **19**, based on the HTNR or H_2TNPG anions, respectively, crystallize isotypically in the triclinic space group *P*−1 with one formula unit per unit cell. Therefore, the compounds' densities differ only slightly (**18c**: 1.805 g cm^{-3} at 101 K, **19**: 1.850 g cm^{-3} at 100 K). Both ECCs show the same octahedral coordination environment with four tetrazole moieties in the equatorial positions and the two anions in the axial position (Figure 11). In case of ECC **18c** parts of the tetrazole and phenyl moieties were split due to disordering. Therefore, parts of the structure were not refined anisotropically. Furthermore, one of the nitrato groups in compound **19** was split. In both structures **18c** and **19**, one of the ethylene groups had to be split because of a disorder.

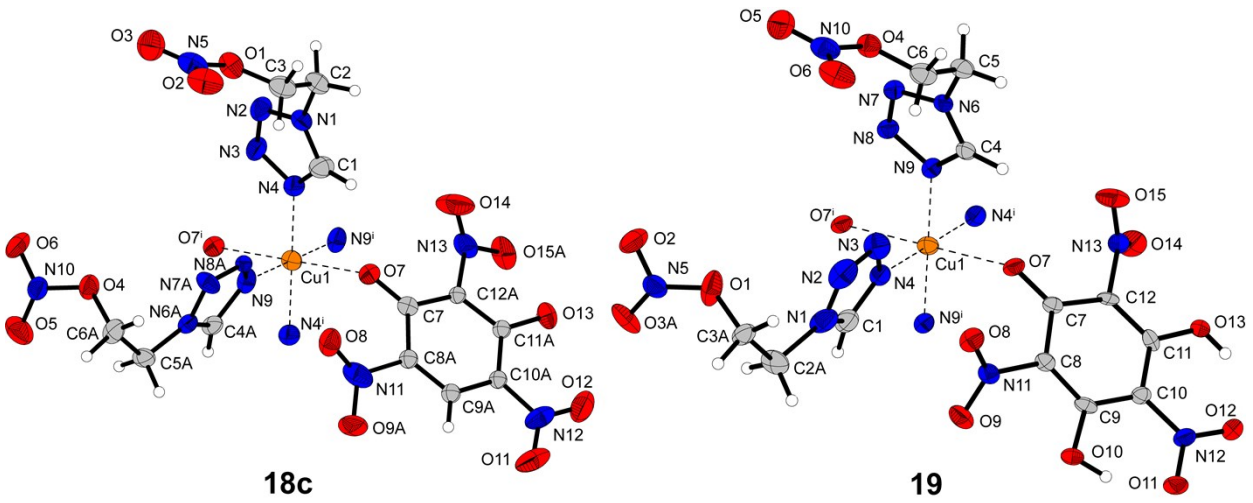

Figure S5. Coordination environment of the complexes [Cu(HTNR)$_2$(1-NET)$_4$] (**18c**) and [Cu(H$_2$TNPG)$_2$(1-NET)$_4$] (**19**). Selected bond lengths (Å) of **18c**: Cu1–O7 2.3844(19), Cu1–N9 2.025(3), Cu1–N4 1.985(2). Selected bond lengths (Å) of **19**: Cu1–O7 2.375(3), Cu1–N4 2.011(3), Cu1–N9 1.991(5). Selected bond angles (°) of **18c**: O7–Cu1–N9 88.83(8), O7–Cu1–N4 85.55(8), N4–Cu1–N9 89.29(10). Selected bond angles (°) of **19**: O7–Cu1–N4 89.14(10), O7–Cu1–N9 85.09(12), N4–Cu1–N9 88.81(16) Symmetry code of **18c**: 1−x, 1−y, 1−z. Symmetry code of **19**: −x, 1-y, 1−z.

The coordination compounds **21** and **22a** based on either a styphnate (TNR^{2-}) or 5-hydroxy-2,4,6-trinitroresorcinate ($HTNPG^{2-}$) anion both crystallize isotypically with similar cell axes and cell volumes in the triclinic space group *P*–1 with two formula units per unit cell. The additional hydroxy group within the $HTNPG^{2-}$ anions leads to an increased density (**21**: 1.935 g cm^{-3} at 102 K, **22a**: 1.970 g cm^{-3} at 102 K). Every complex shows a distorted octahedral coordination sphere with two ligand moieties in equatorial positions (Figure 12). The remaining equatorial coordination sites are occupied by deprotonated hydroxy groups of the trinitrophenolate ion. The axial positions are taken by nitro groups of the anion, which are closest to the binding hydroxy groups. The binding behaviour of the respective anion leads to the formation of one-dimensional polymeric chains.

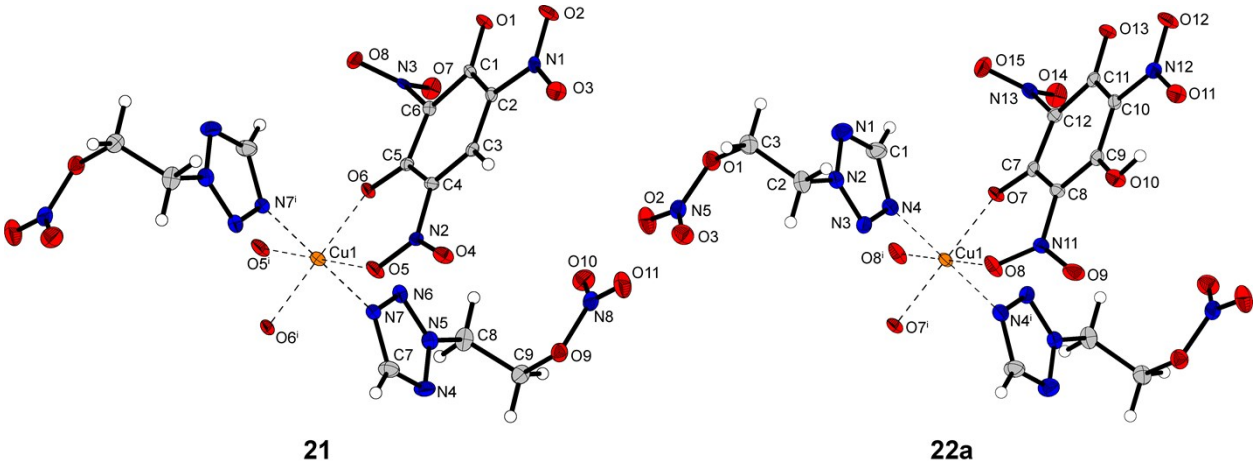

Figure S6. Coordination environments of the complexes $[Cu(2\text{-}NET)_2(TNR)]$ (**21**) and $[Cu(HTNPG)(2\text{-}NET)_2]$ (**22a**). Selected bond lengths (Å) of **21**: Cu1–O6 1.942(2), Cu1–O5 2.258(3), Cu1–N7 2.022(3). Selected bond lengths (Å) of **22a**: Cu1–O7 1.9473(16), Cu1–N4 2.027(2), Cu1–O8 2.2396(17). Selected bond angles (°) of **21**: O5–Cu1–O6 83.71(9), N7–Cu1–O5 89.93(11), O6–Cu1–N7 88.93(11). Selected bond angles (°) of **22a**: O8–Cu1–O7 82.71(7), O8–Cu1–N4 86.46(8), O7–Cu1–N4 88.63(8). Symmetry code of **21**: (i) 1–x, 2–y, –z. Symmetry code of **22a**: (i) –x, 1–y, 1–z.

ECC **22c** crystallizes in the triclinic space group *P*−1 in the form of green platelets and the unit cell consists of one formula unit. The compound possesses a calculated density of 1.803 g cm^{-3} at 123 K, which is the lowest observed value for all trinitrophenolate complexes based on 2-NET (**5**). The coordination sphere is built up like the 1-NET based complex **19**. Four tetrazole moieties are arranged in the equatorial positions together with anions occupying the axial spots. The major difference to **19**, or **22b**, is that two additional, non-coordinating 2-NET moieties are located within the molecular unit (Figure 13). This behaviour has not been observed among copper complexes based on the H_2TNPG anion. It is likely due to the alkyl chain length of the ligand, allowing the ligand to perfectly fit into the free spots of the structure. This is also favoured by two different conformations of the C–C bond, which were observed within the structure. The co-crystallizing ligand, together with two of the equatorial ligands show a *gauche* conformation (N10–C11–C12–O1= 58.4(4)°, N15–C14–C15–O16 = 50.1(3)), whereas the remaining two ligands are arranged in an *anti*-conformation (N5–C8–C9–O10 = 172.40(18)°).

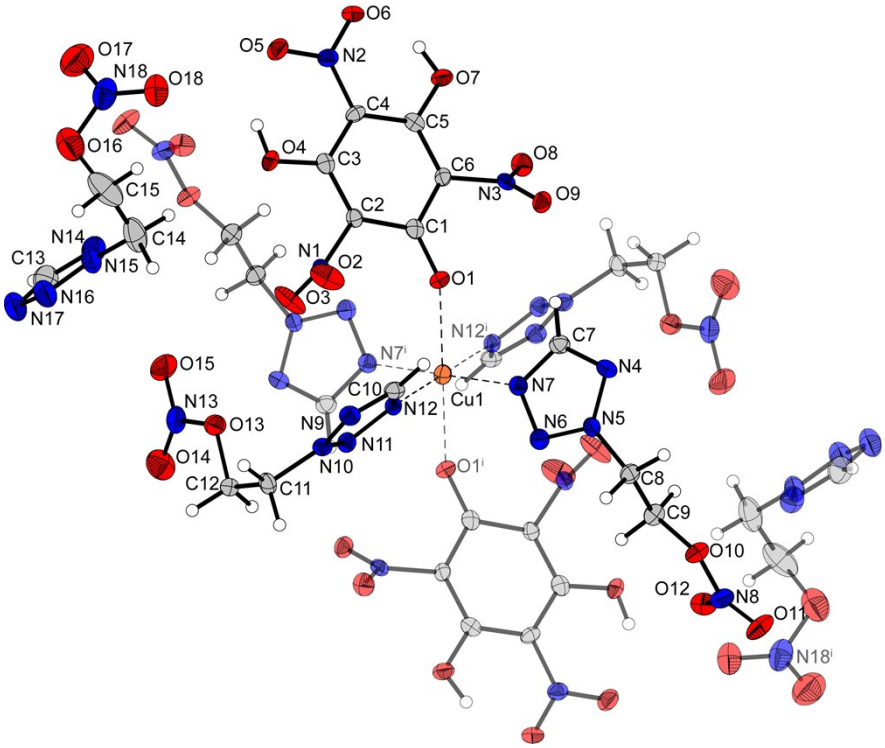

Figure S7. Molecular unit of [Cu(H_2TNPG)$_2$(2-NET)$_4$] • 2 2-NET (**22c**). Selected bond lengths (Å): Cu1–O1 2.317(2), Cu1–N7 2.006(2), Cu1–N12 2.043(3). Selected bond angles (°): O1–Cu1–N7 84.11(11), O1–Cu1–N12 88.70(11), N7–Cu1–N12 88.71(11). Symmetry code: 1−x, 1−y, 1−z.

3. Computations & Hishfeld Surfaces

3.1 Computations

All calculations were carried out using the Gaussian G09 program package.[S13] The enthalpies (H) and free energies (G) were calculated using the complete basis set (CBS) method of Petersson and coworkers in order to obtain very accurate energies. The CBS models use the known asymptotic convergence of pair natural orbital expressions to extrapolate from calculations using a finite basis set to the estimated complete basis set limit. CBS-4 begins with a HF/3-21G(d) geometry optimization; the zero point energy is computed at the same level. It then uses a large basis set SCF calculation as a base energy, and a MP2/6-31+G calculation with a CBS extrapolation to correct the energy through second order. A MP4(SDQ)/6-31+(d,p) calculation is used to approximate higher order contributions. In this study we applied the modified CBS-4M method (M referring to the use of minimal population localization) which is a re-parametrized version of the original CBS-4 method and also includes some additional empirical corrections. The enthalpies of the gas-phase species M were computed according to the atomization energy method (E 1) (Table S7 & 8).[S13–18]

$$\Delta_f H^\circ_{(g,\,M,\,298)} = H_{(Molecule,\,298)} - \sum H^\circ_{(Atoms,\,298)} + \sum \Delta_f H^\circ_{(Atoms,\,298)} \qquad (E1)$$

Table S7. Literature values for atomic $\Delta H^\circ_f{}^{298}$ / kcal mol^{-1}

	$-H^{298}$ [a.u.]	NIST[S19]
H	0.50091	52.1
C	37.786156	171.3
N	54.522462	113.0
O	74.991202	59.6

In the last step the gas-phase heat of formations were converted to the solid/liquid state ones by subtracting the vaporization/sublimation enthalpies (calculated using the Trouton rule).[S20,21] The calculation results are summarized in Table S8.

Table S8. CBS-4M results, Gas phase enthalpies of formation, calculated sublimation/vaporization enthalpies and solid-state heat of formation.

Compound	$-H^{298}$ / a.u.	$\Delta_f H°$(g) / kJ mol^{-1}	$\Delta H°$(sub/vap) / kJ mol^{-1}	$\Delta_f H°$(s) / kJ mol^{-1}
4	−615.780788	229.8	56.0522	173.7
5	−615.790916	203.2	56.0522	147.1
TNT	–	–	–	−59.346

3.2 Hirshfeld Surfaces

Hirshfeld surfaces of compound **4** and **5** were generated from the crystal structure data with CrystalExplorer17.[S22] Fingerprint plots are shown in Figure S5. Interactions are represented by dots in the fingerprint plot and corresponding distances can be calculated by the addition of the distance d_e and d_i. Therefore, the area in the lower left represents close interactions. These close interactions, attractive or repulsive, are represented by red dots on the Hirshfeld surface.

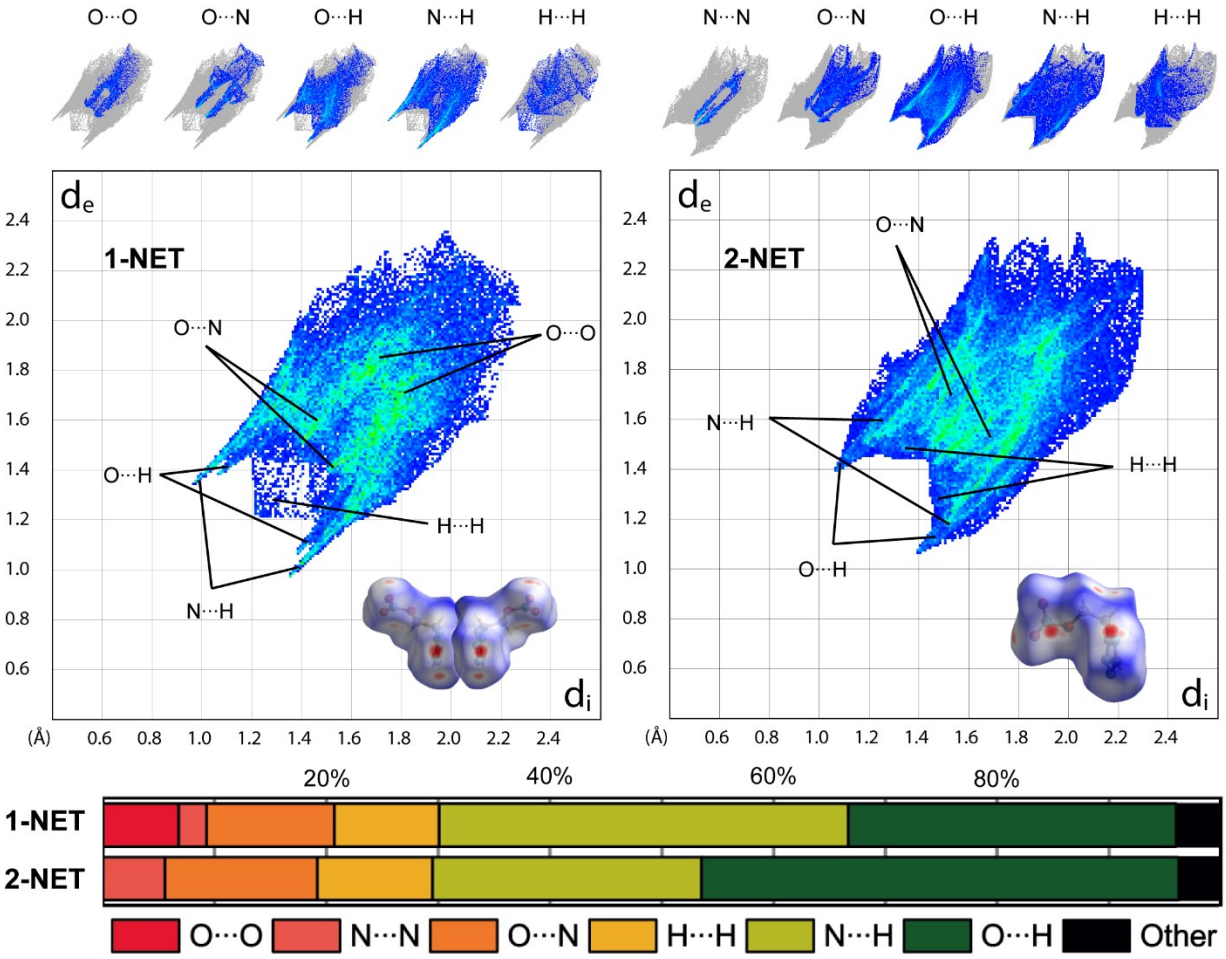

Figure S8. Two-dimensional fingerprint plots of **4** and **5** together with their Hirshfeld surfaces. The areas of the single interactions are represented above the graphs.

4. NMR Spectroscopy of 4 and 5

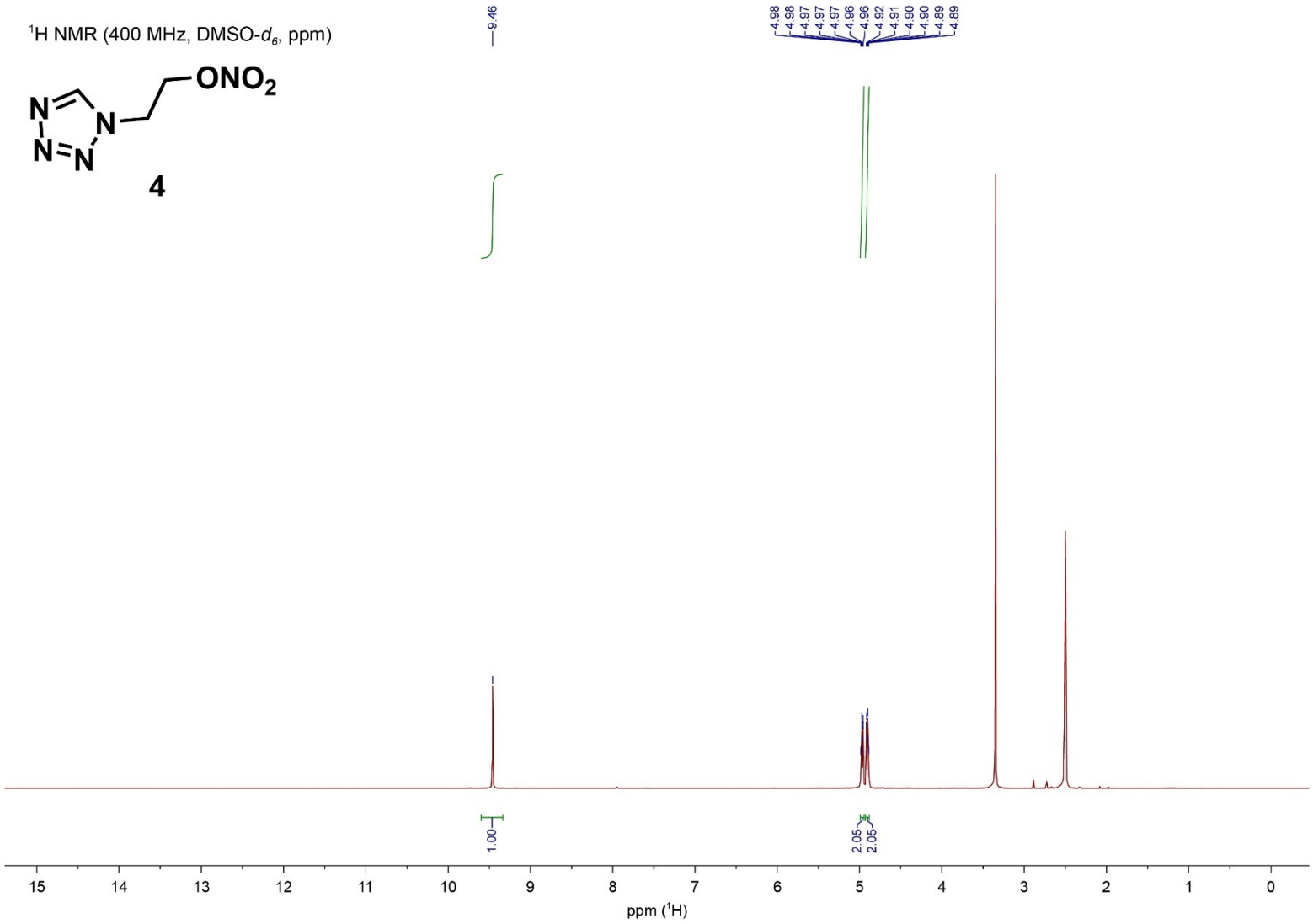

Figure S9. ^{1}H NMR spectrum of 1-NET (**4**).

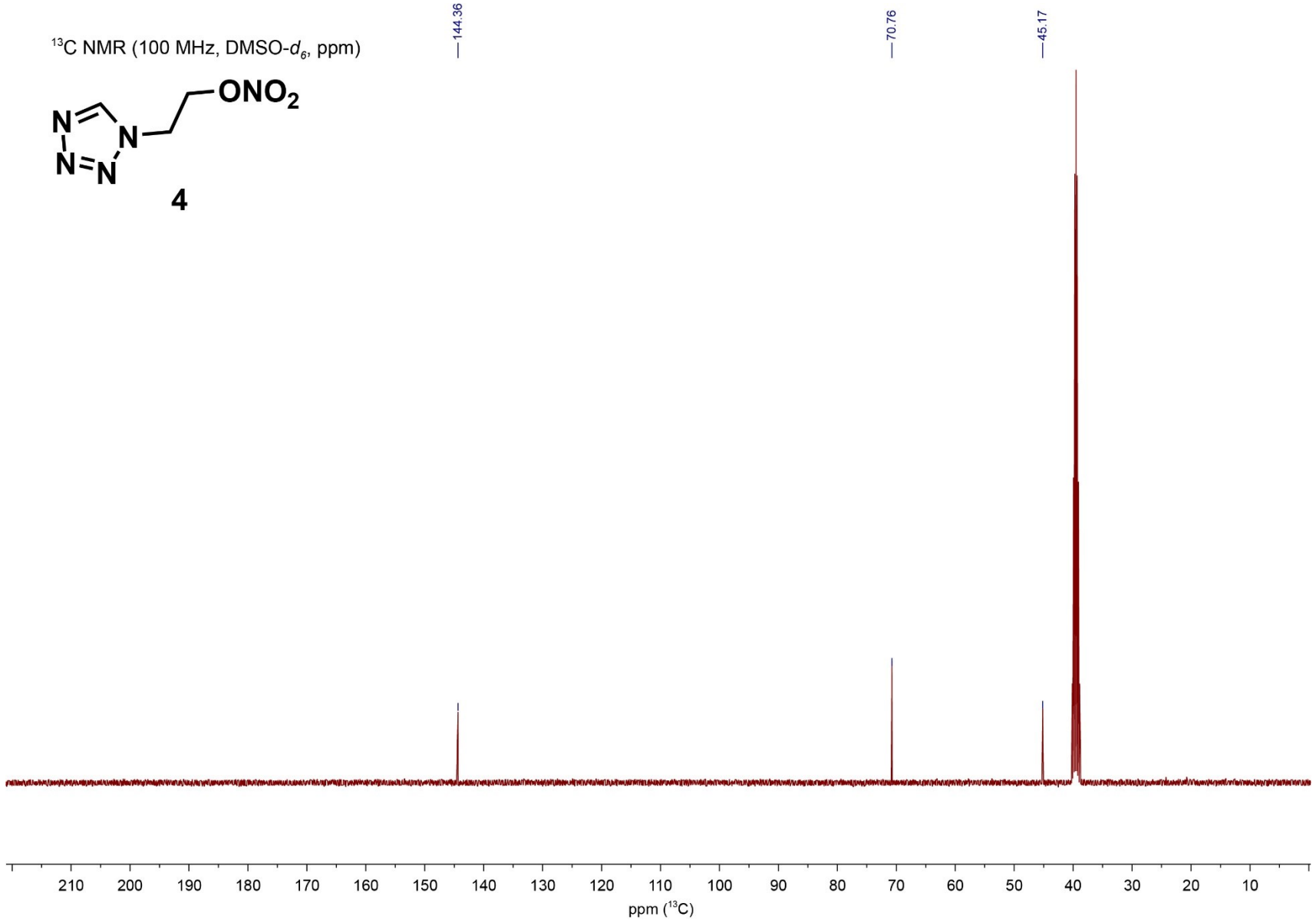

Figure S10. ^{13}C NMR spectrum of 1-NET (**4**).

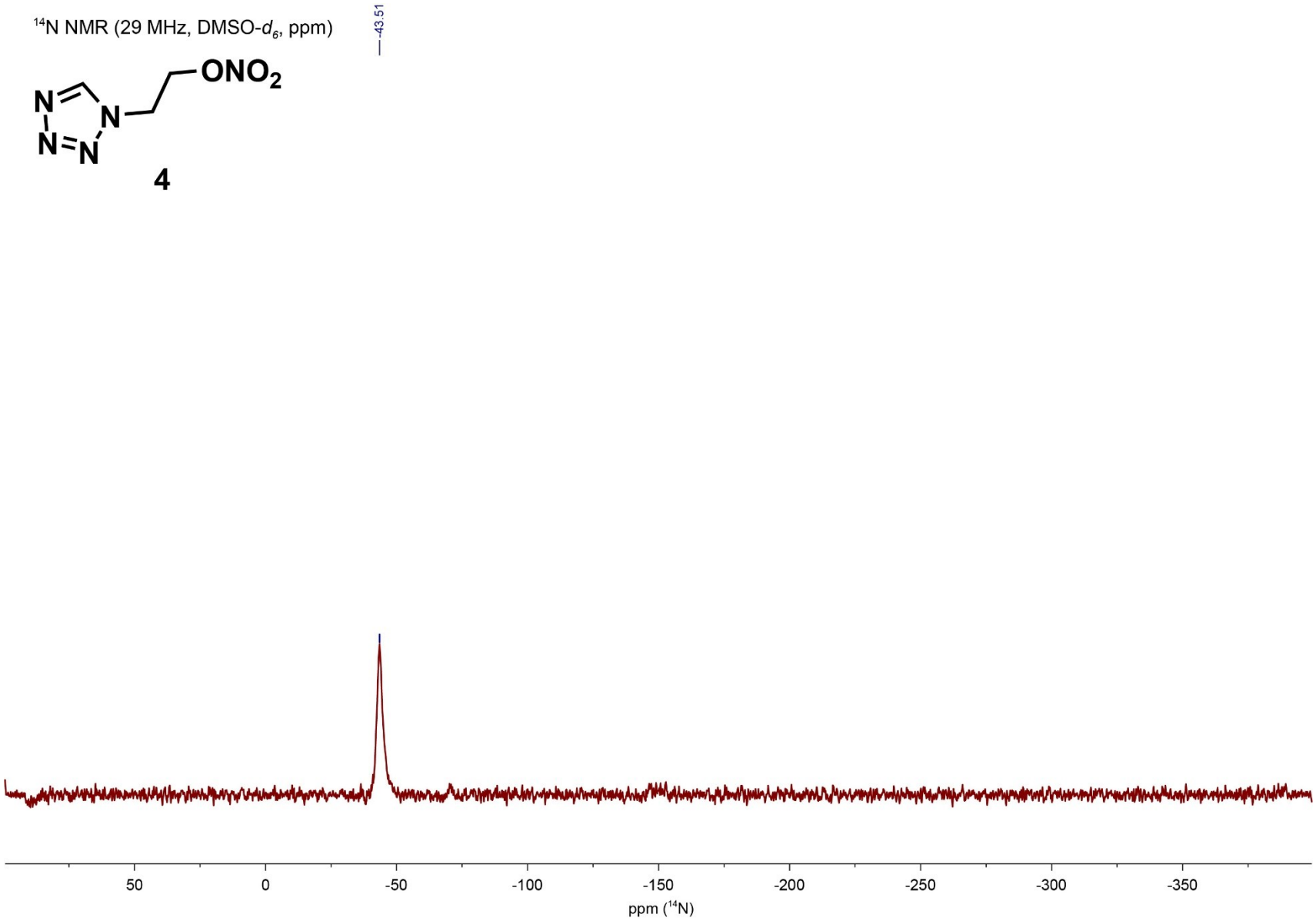

Figure S11. ^{14}N NMR spectrum of 1-NET (**4**).

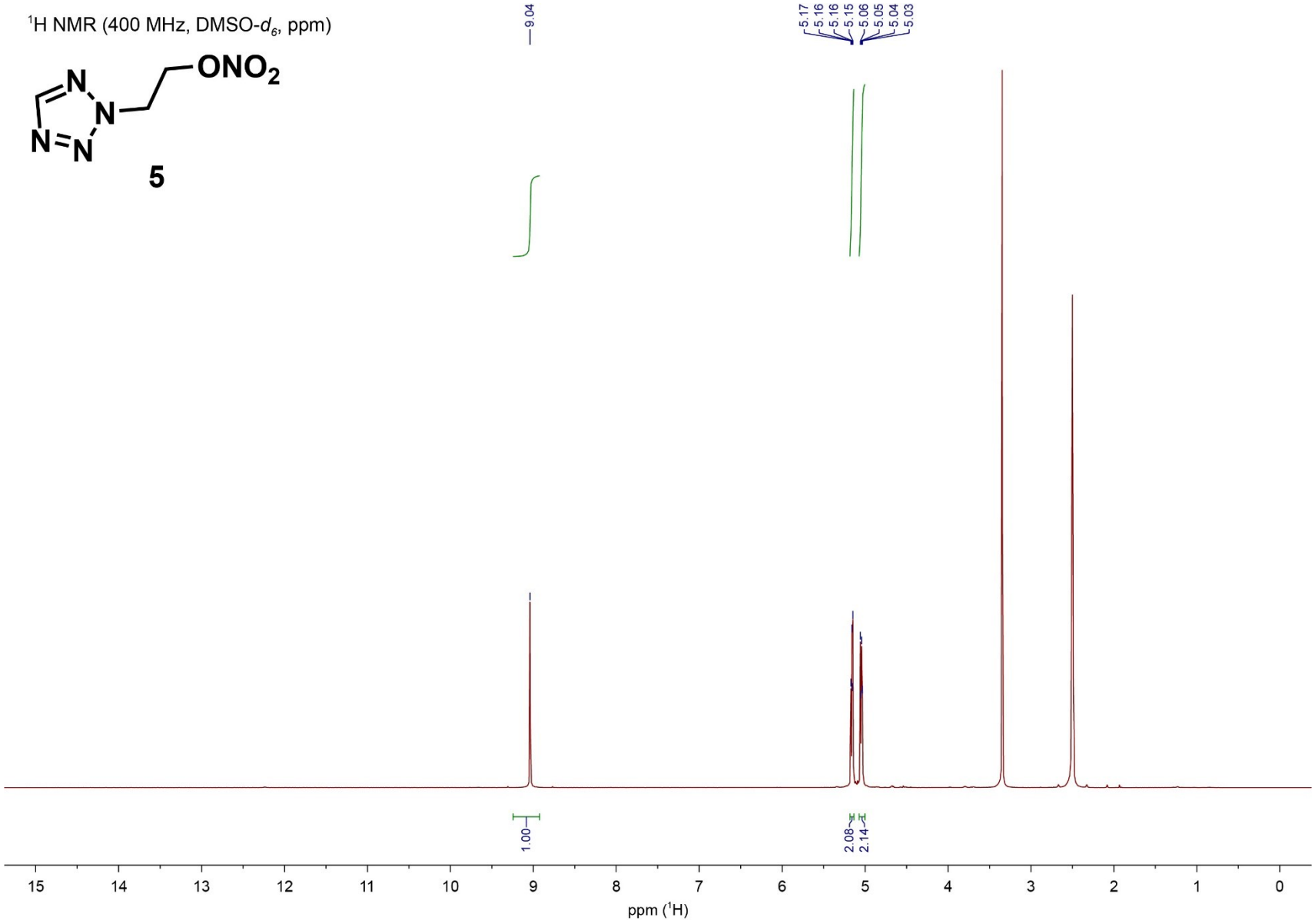

Figure S12. [1]H NMR spectrum of 2-NET (**5**).

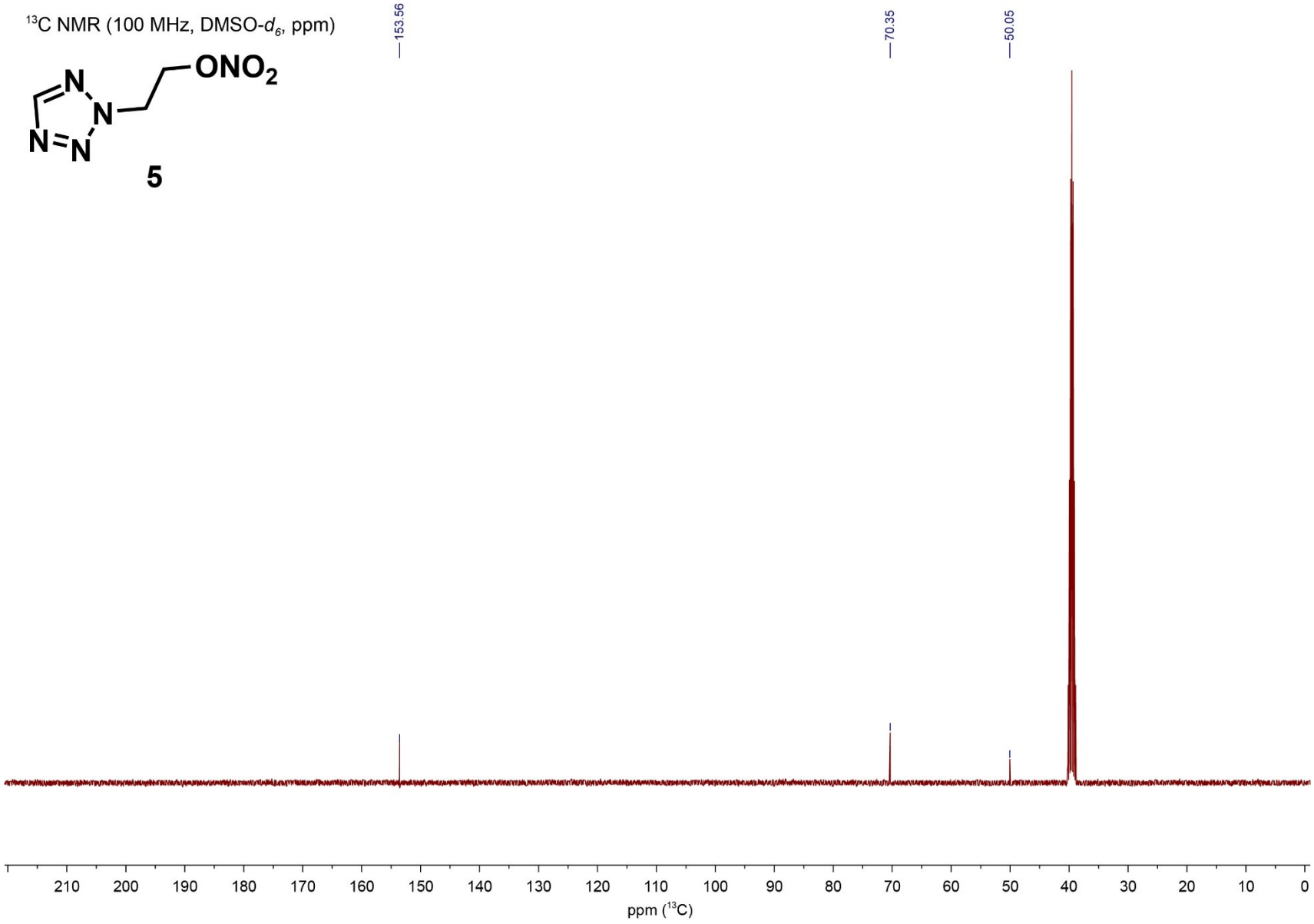

Figure S13. ^{13}C NMR spectrum of 2-NET (**5**).

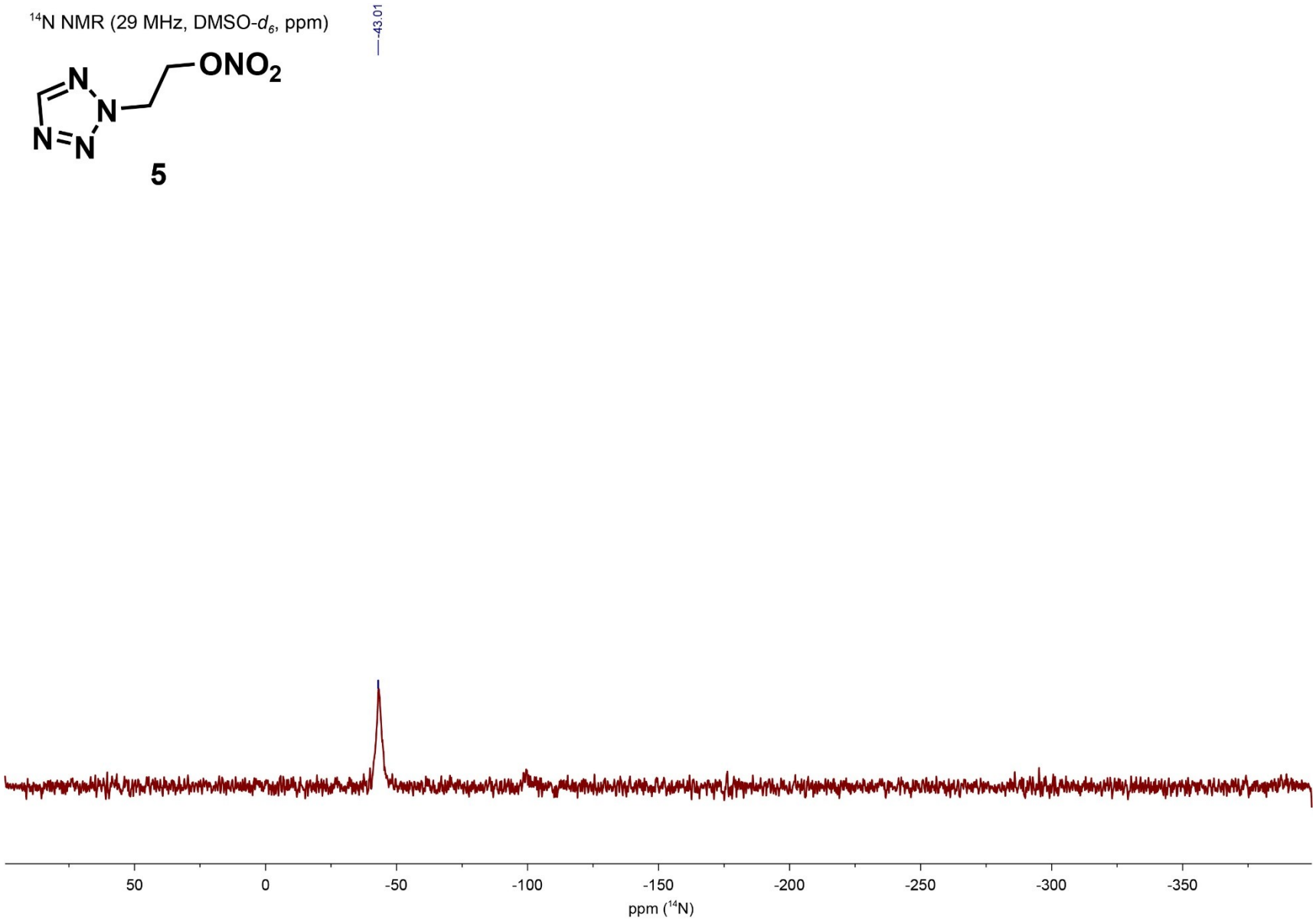

Figure S14. ^{14}N NMR spectrum of 2-NET (**5**).

4. IR Spectroscopy of 1, 2, 4–9, 11, 13, 14, and 16–22

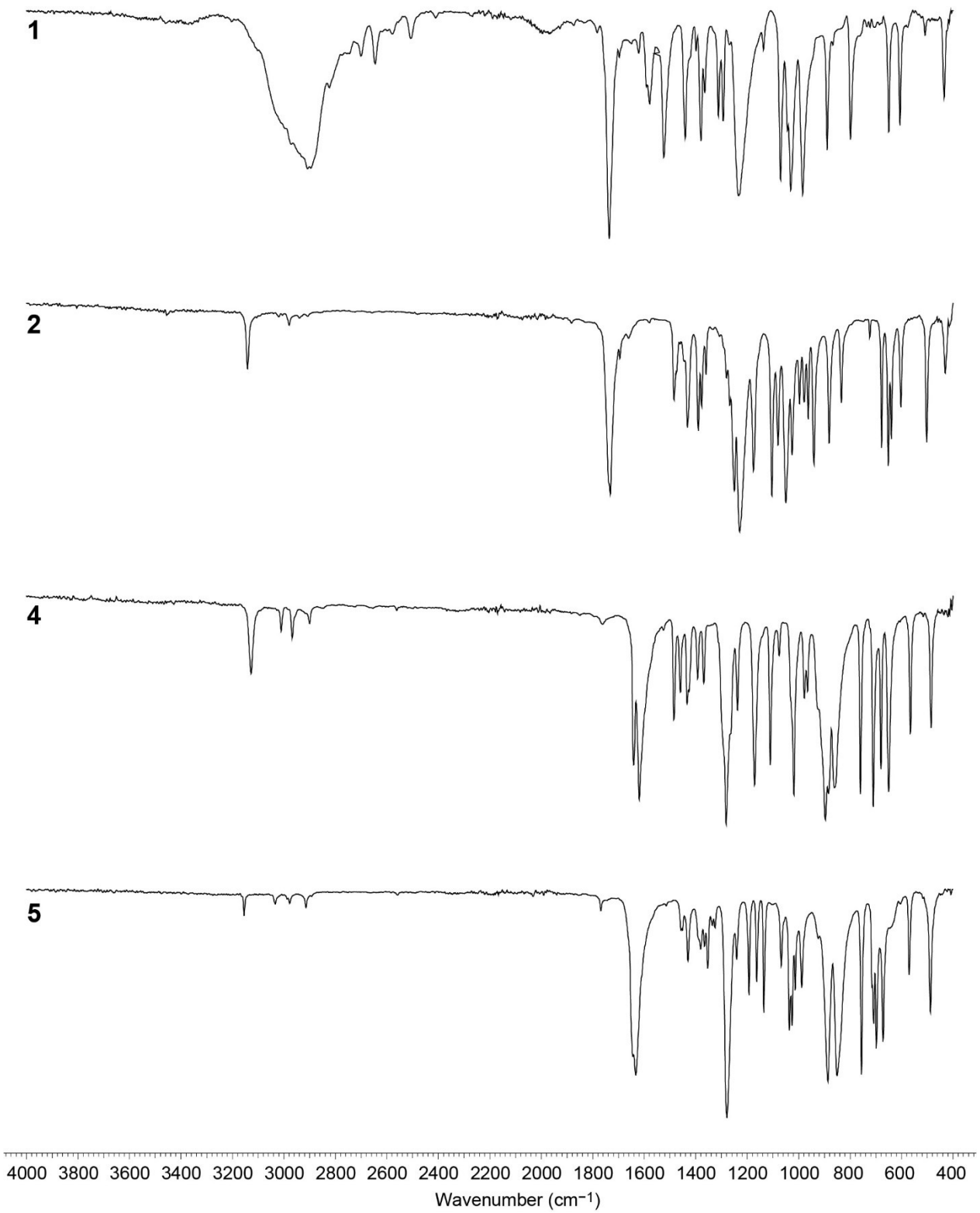

Figure S15. IR spectra of the organic molecules **1**, **2**, **4**, and **5**.

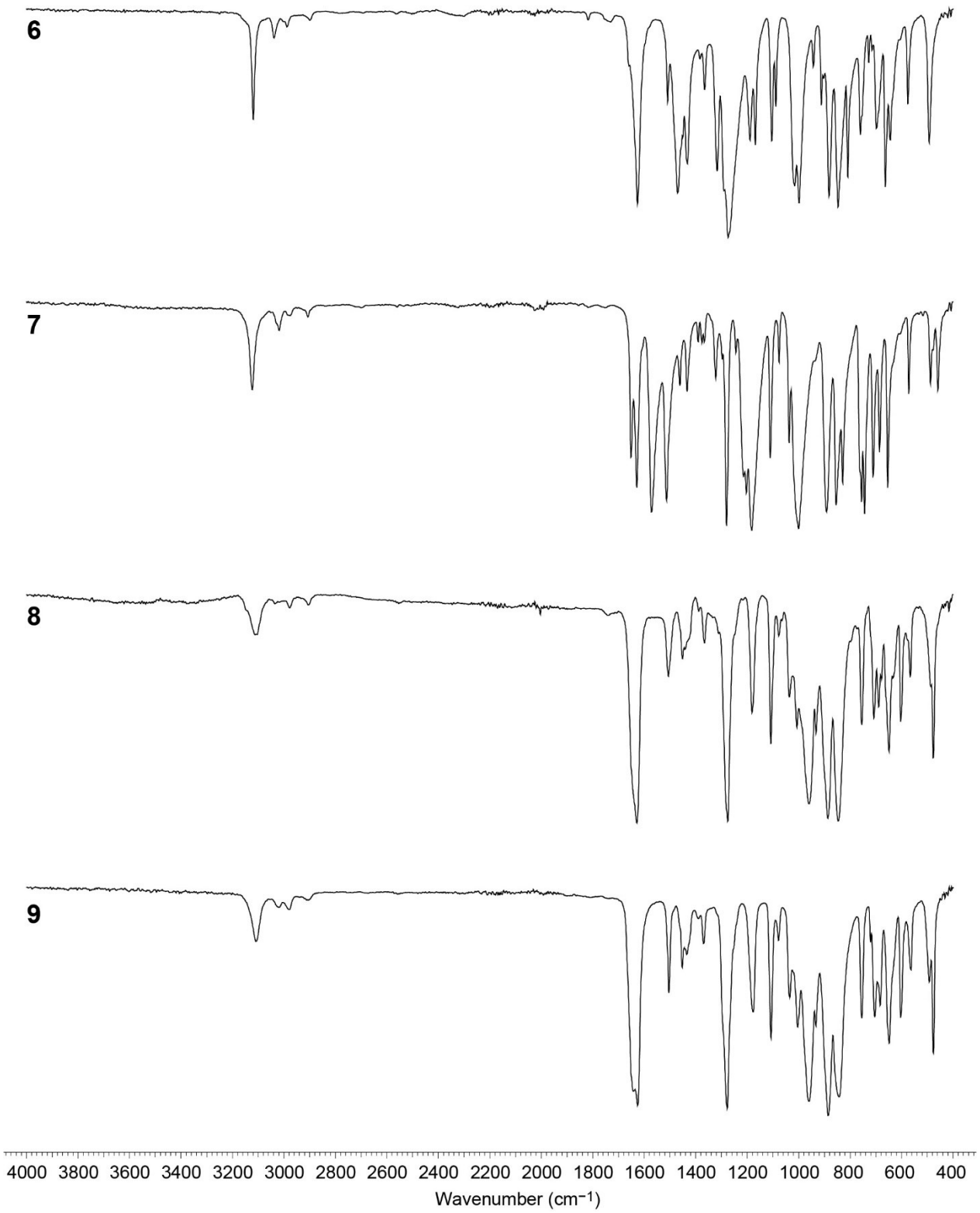

Figure S16. IR spectra of the complexes **6**–**9**.

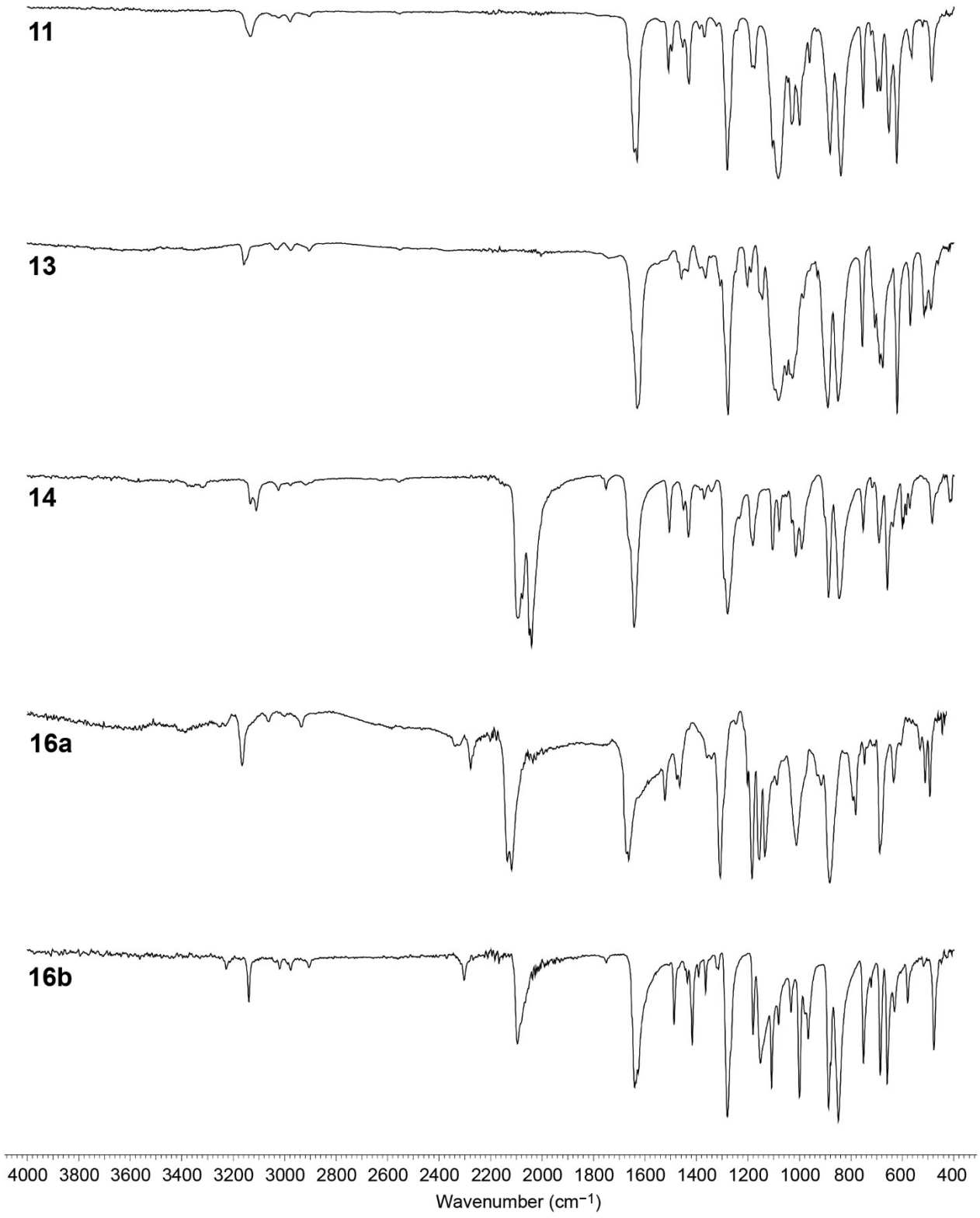

Figure S17. IR spectra of the ECC **11**, **13**, **14**, and **16a**–**b**.

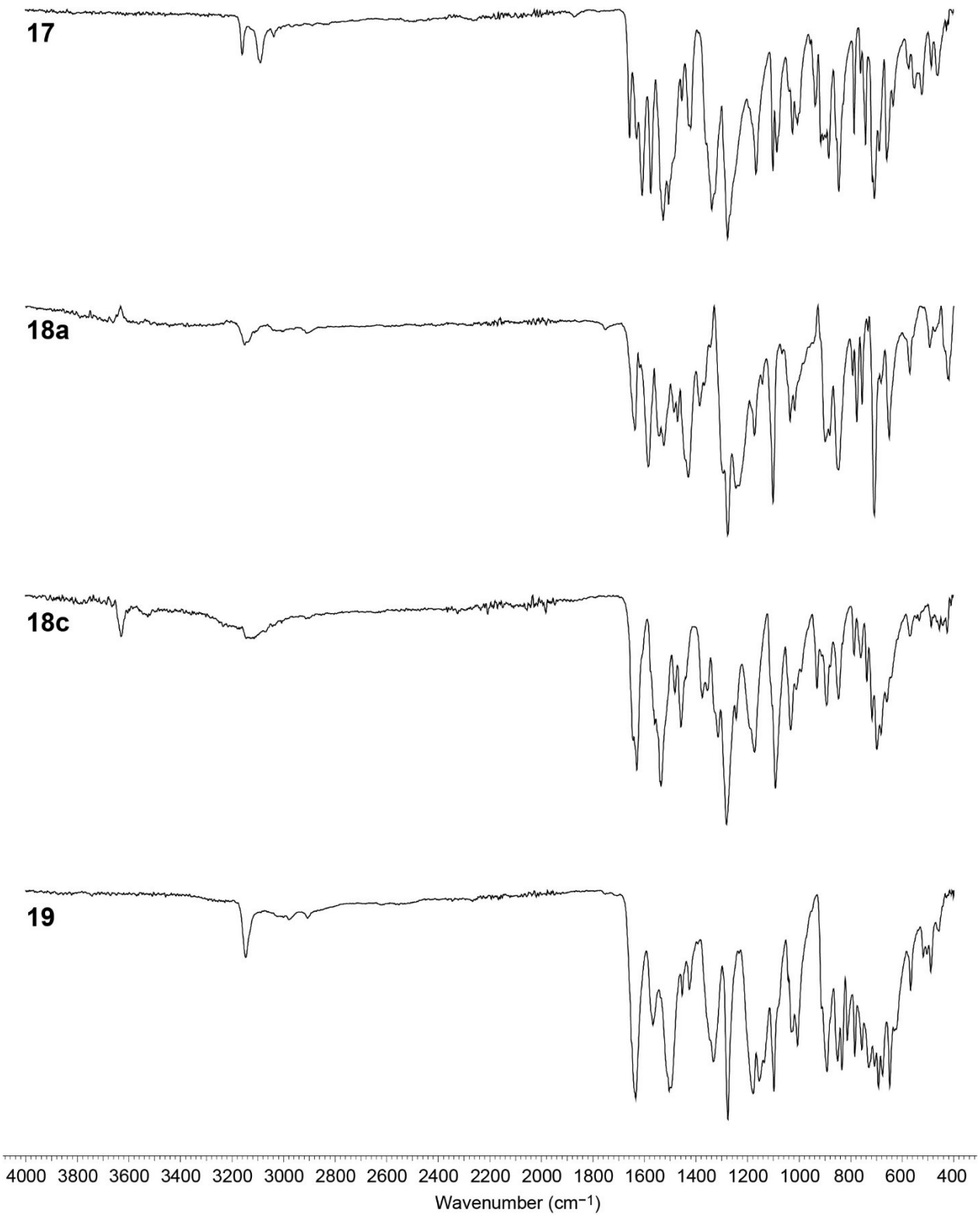

Figure S18. IR spectra of the coordination compounds **17–19** based on various trinitrophenolate anions.

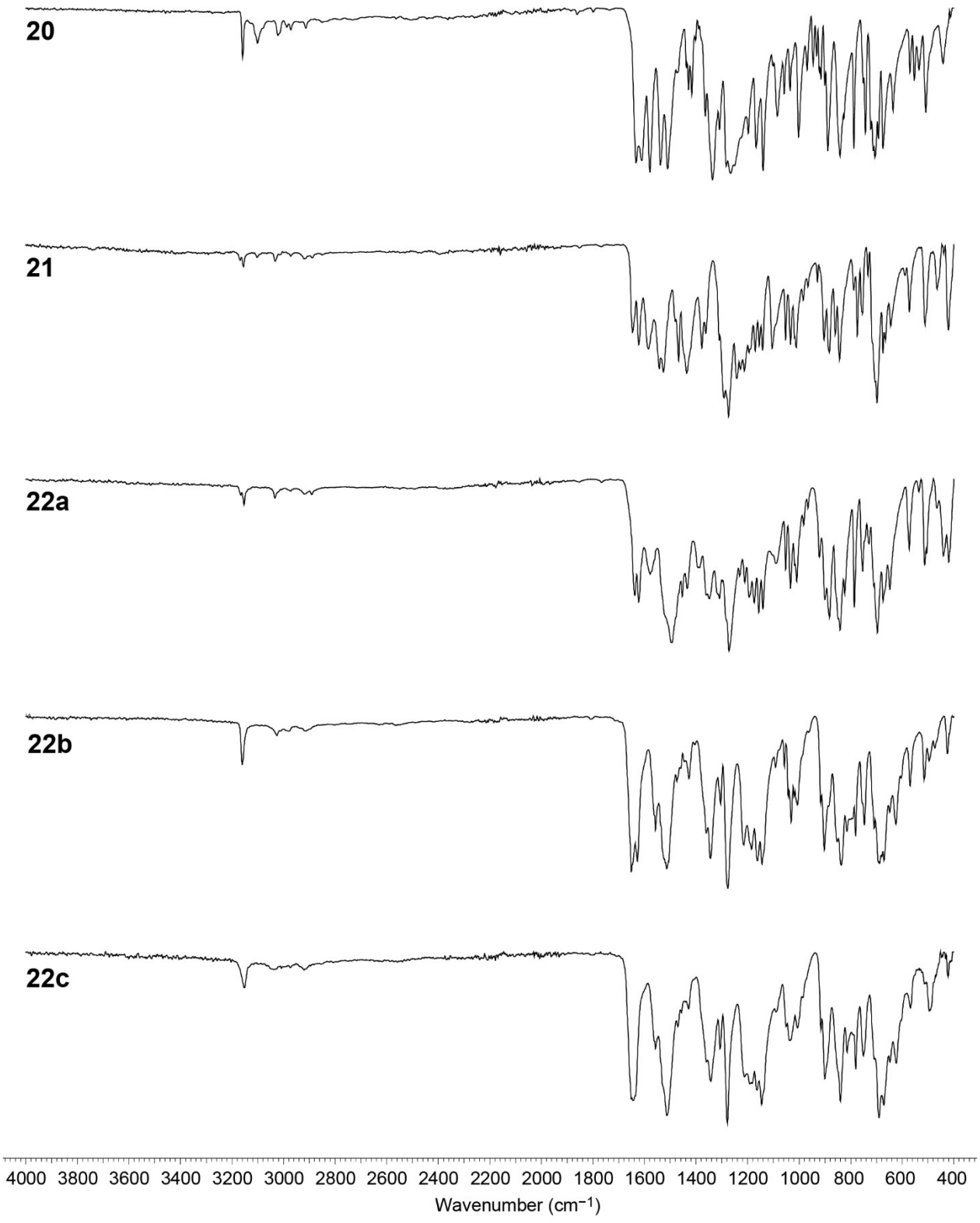

Figure S19. IR spectra of the coordination compounds **20**–**22**.

5. DTA Plots of 4–9, 11, 13, 14, and 16–22

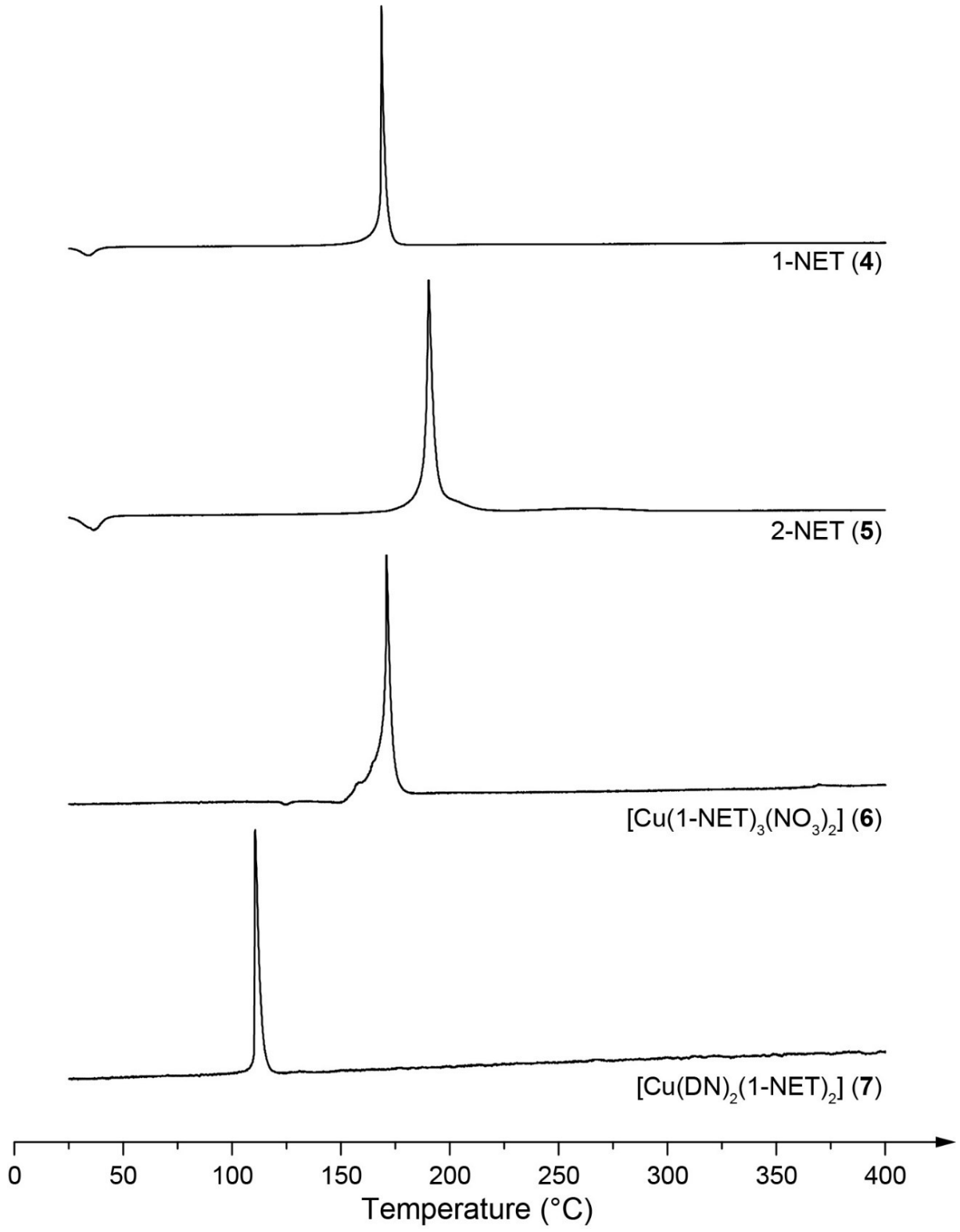

Figure S20. DTA plots of the ligands **4** and **5** together with the complexes **6** and **7**.

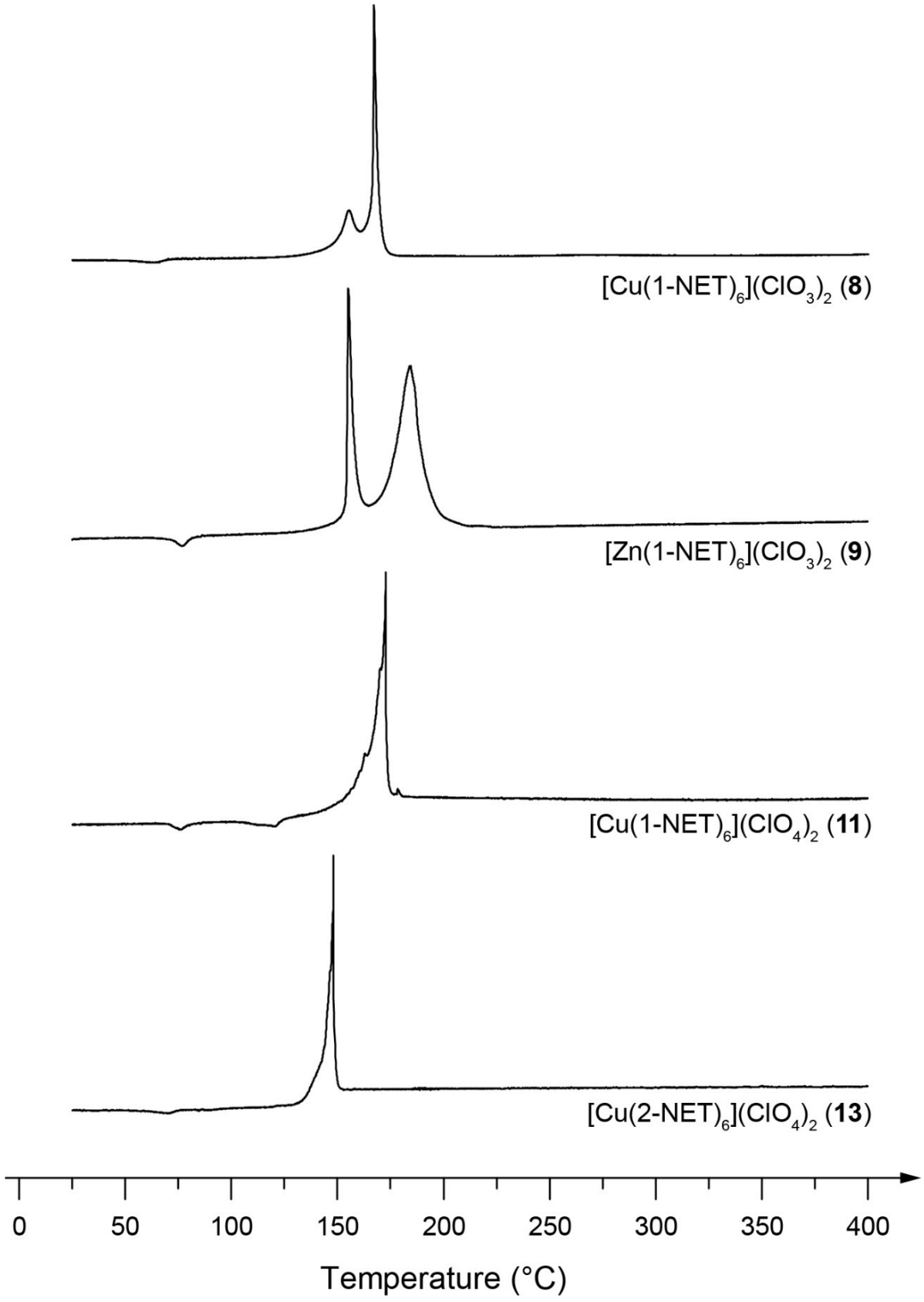

Figure S21. DTA measurements of the compounds **8**, **9**, **11**, and **13**.

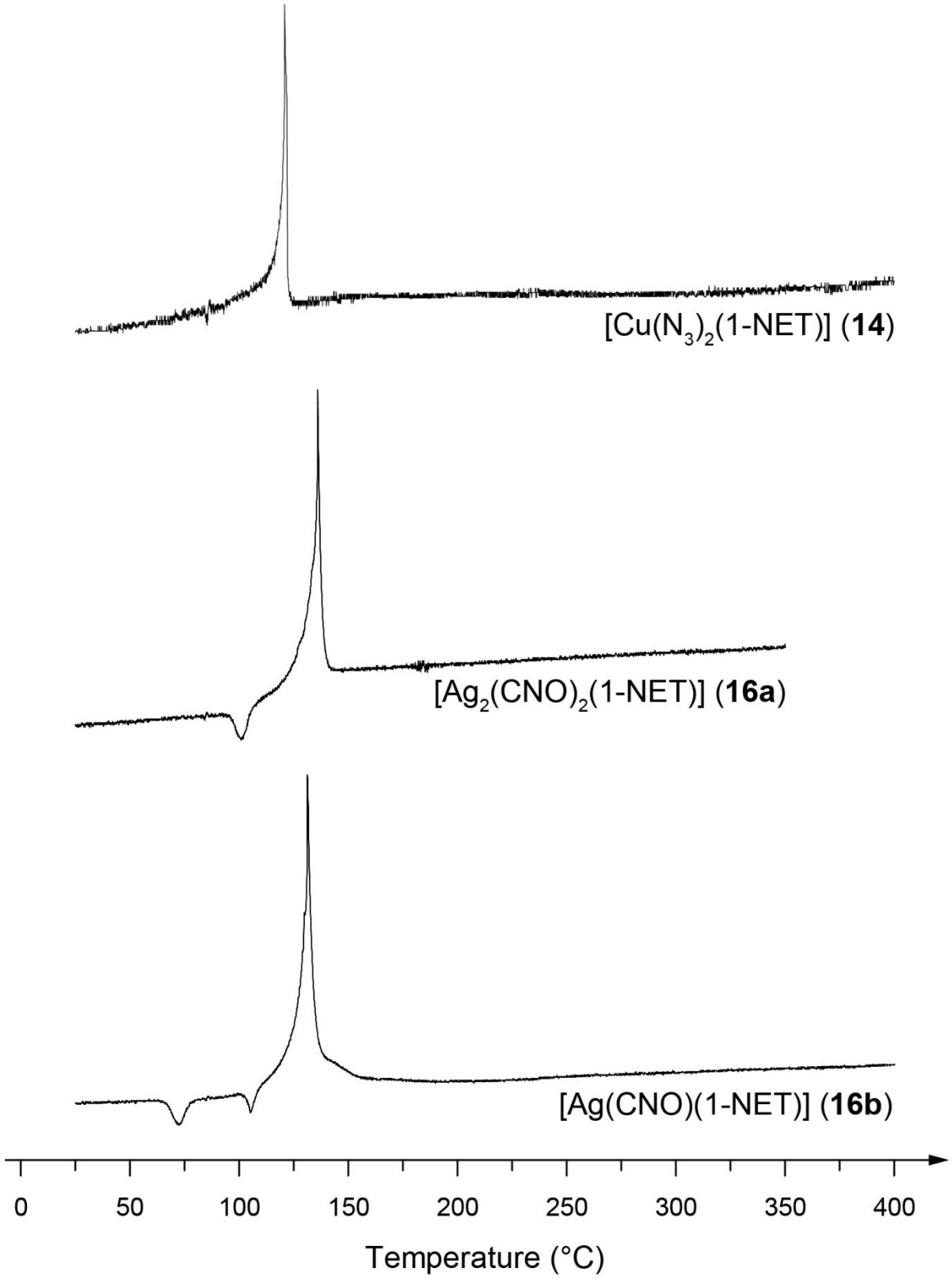

Figure S22. DTA measurements of the ccomplexes **14**, **16a**, and **16b**.

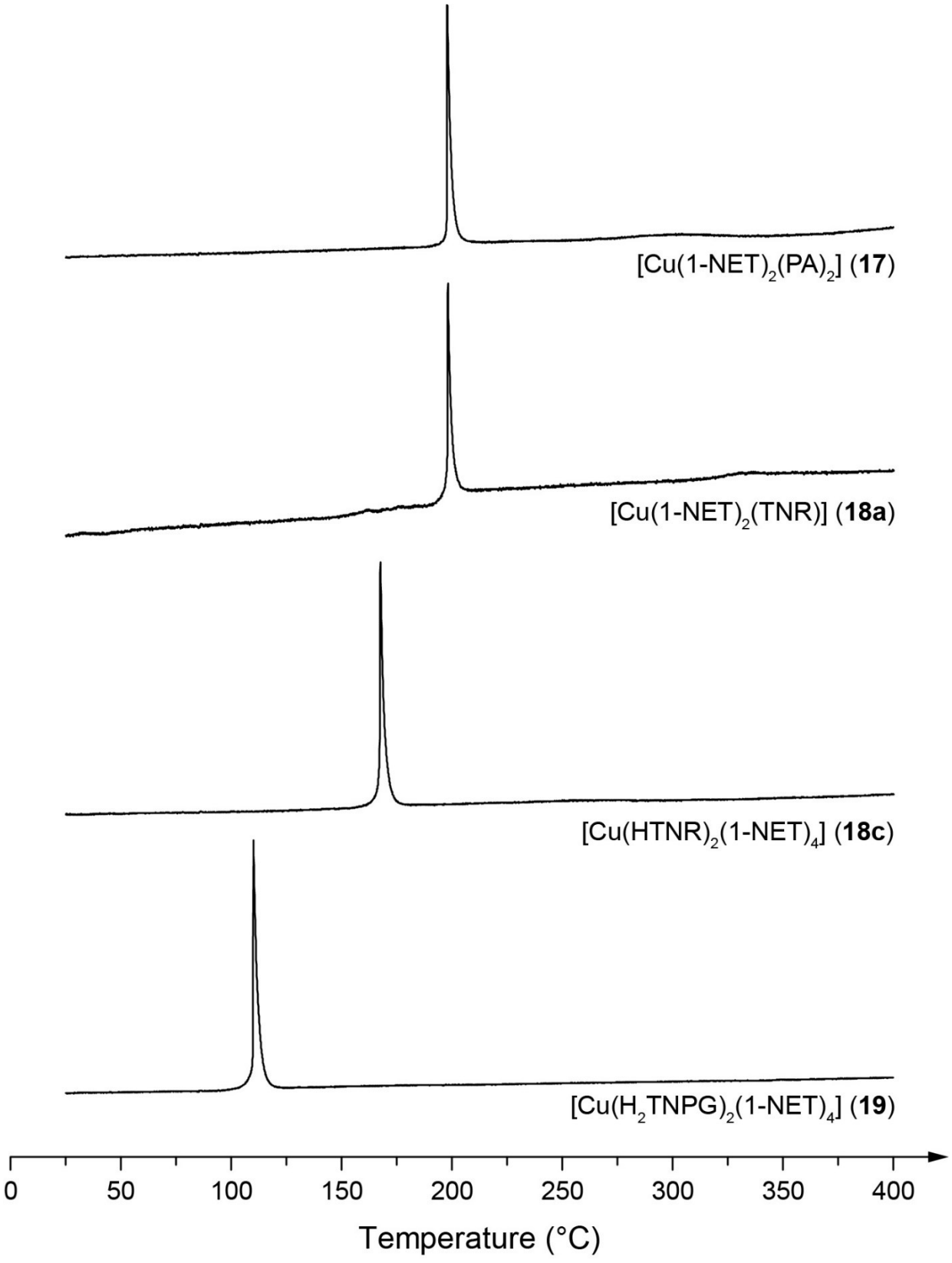

Figure S23. DTA measurements of the trinitrophenolate-based complexes **17**–**19**.

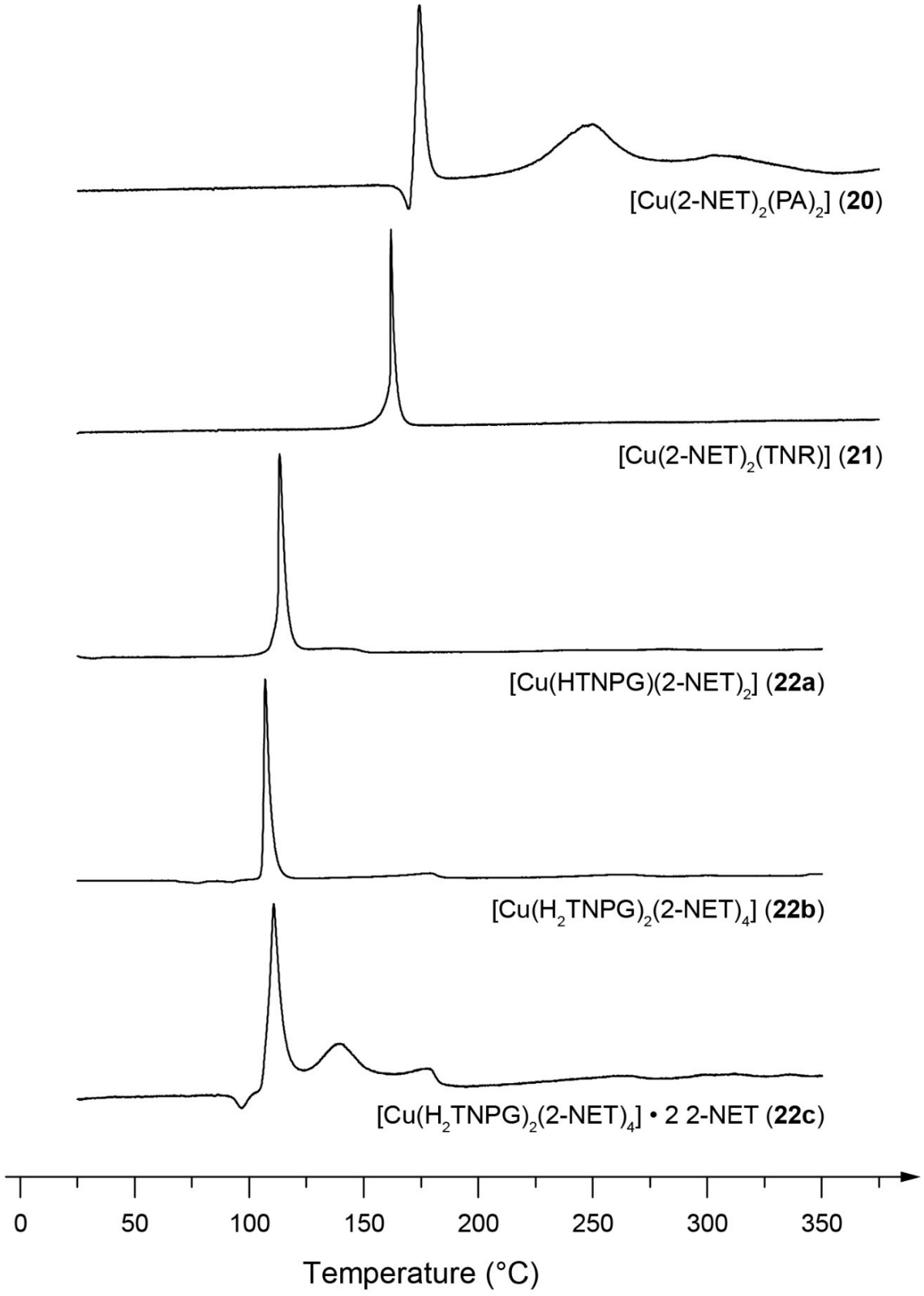

Figure S24. DTA measurements of the trinitrophenolate-based complexes **20**–**22**.

6. TGA Plots of 4–6, 8, 9, 11, 13, 16, 20, and 22

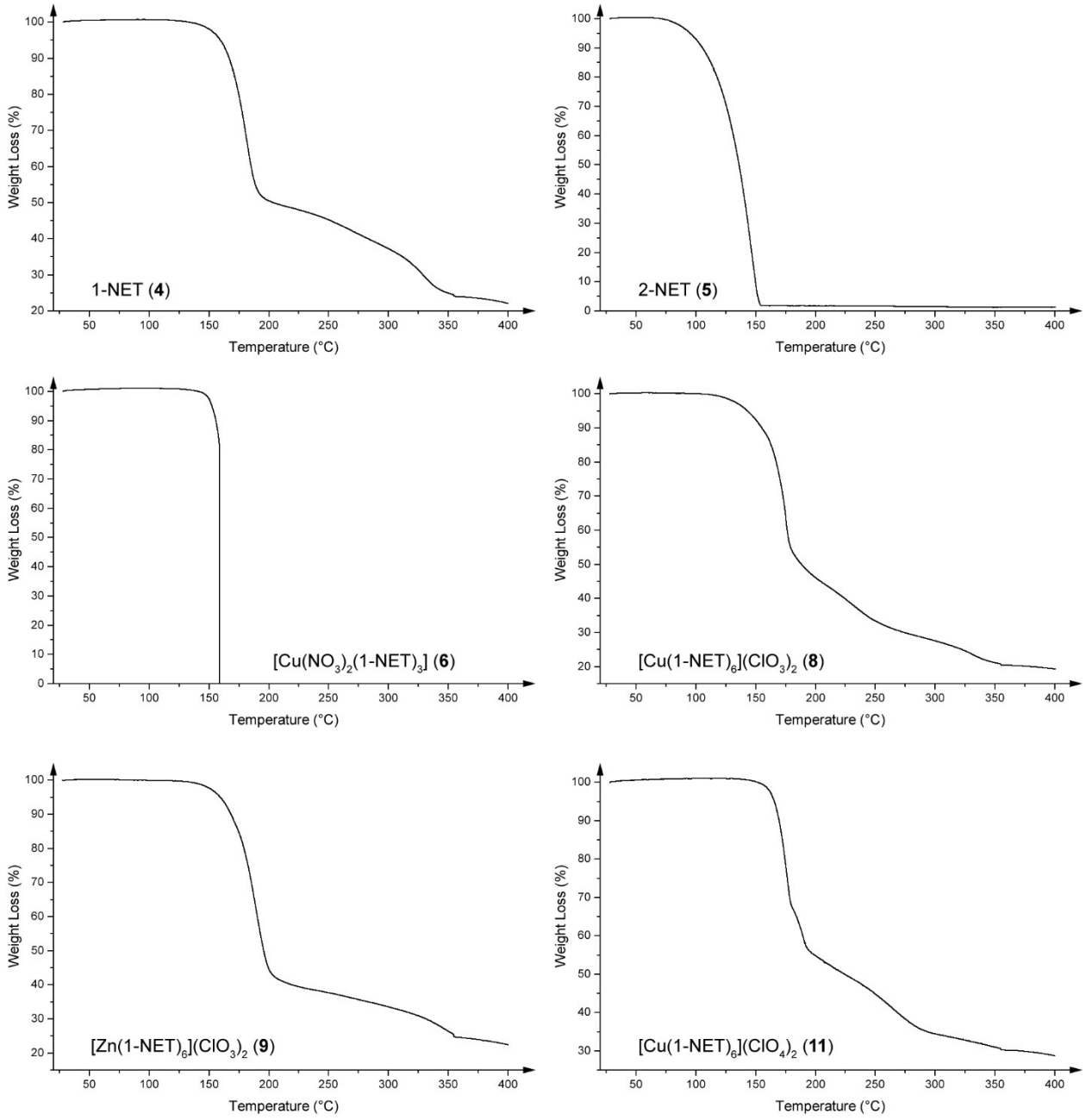

Figure S25. TG measurements of the ligands **4** and **5** together with the complexes **6**, **8**, **9**, an **11**.

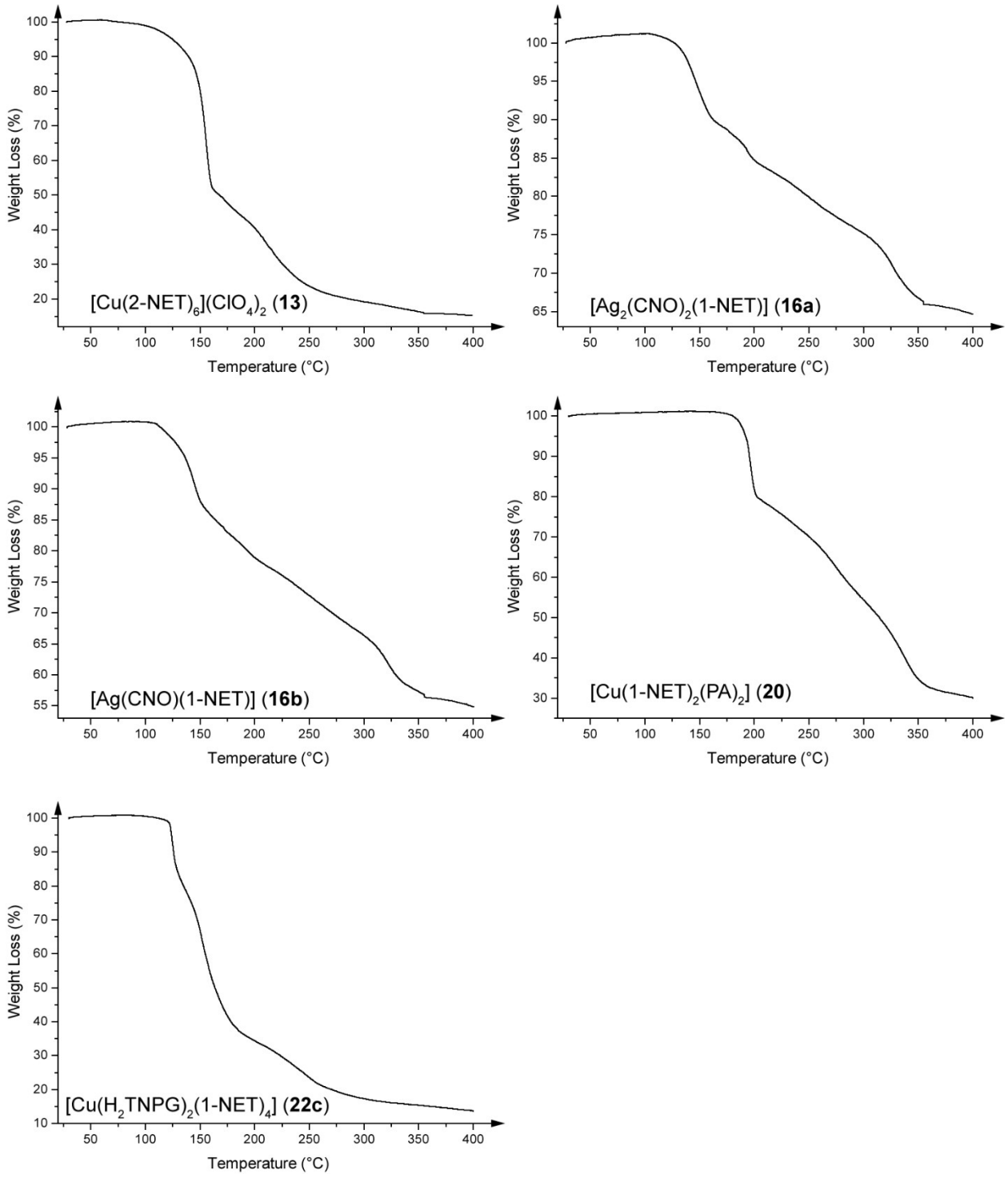

Figure S26. TGA plots of the ECCs **13**, **16a**, **16b**, **20**, and **22c**.

7. Hot Plate & Hot Needle Tests of 6–9, 11, 13, 14, 16–22

Figure S27. Deflagration of the nitrato complex **6** during hot plate (left) and hot needle test (right).

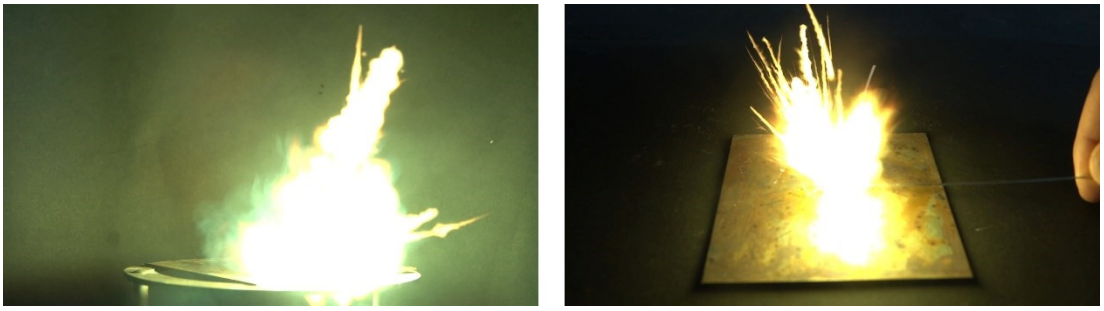

Figure S28. Reaction of the dinitramide complex **7** during hot plate (left) and hot needle test (right).

Figure S29. Deflagration reaction of ECC **8** during hot plate (left) and hot needle test (right).

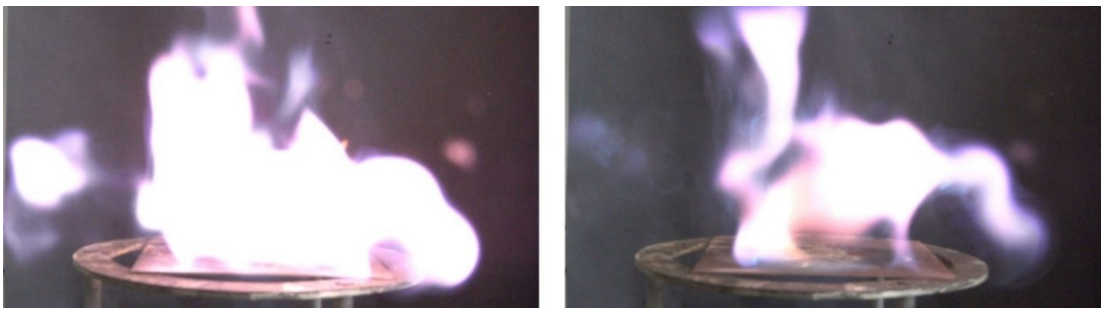

Figure S30. Deflagration of the zinc chlorate complex **9** during hot plate test.

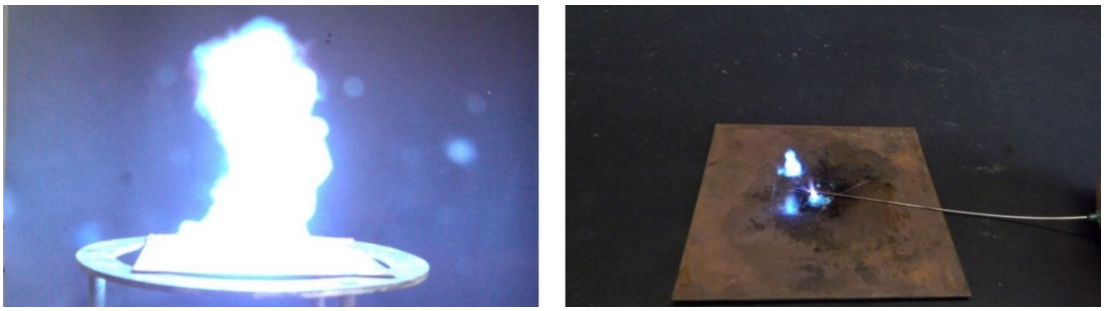

Figure S31. Reaction of the coordination compound **11** during hot plate (left) and hot needle test (right).

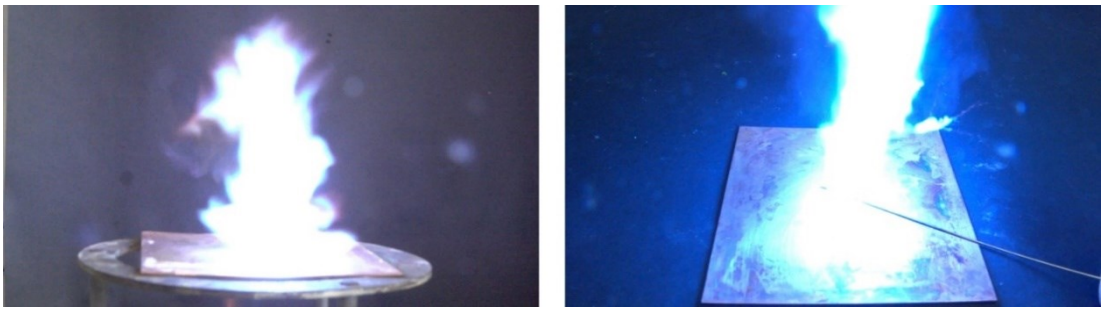

Figure S32. Results of the hot plate (left) and hot needle tests (right) of the ECC **13**.

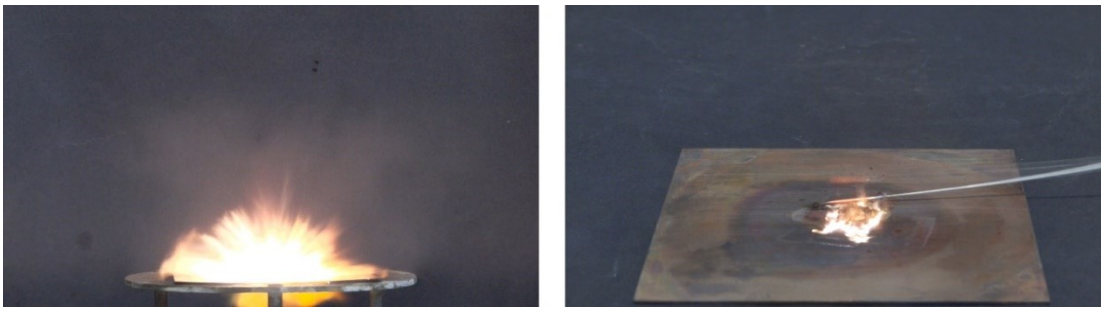

Figure S33. Detonations of the copper azide complex **14** during hot plate (left) and hot needle test (right).

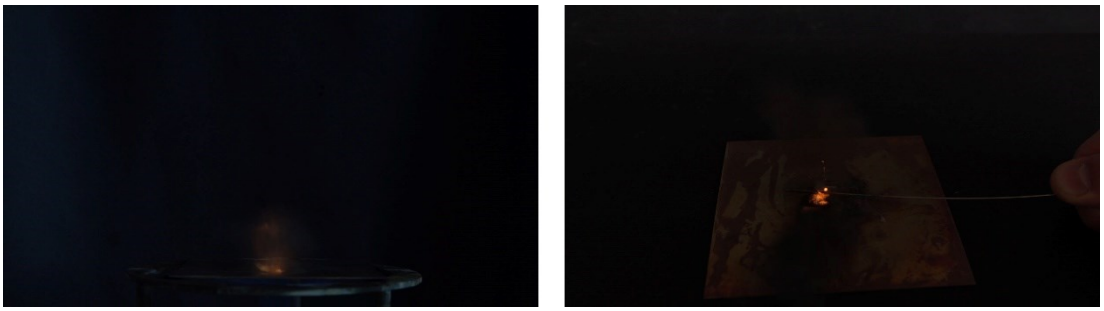

Figure S34. Detonations of the silver fulminate complex **16a** during hot plate (left) and deflagration during hot needle test (right).

Figure S35. Reactions of the coordination compound **16b** during hot plate (left) and hot needle test (right).

Figure S36. Deflagration of the picrate complex **17** during hot plate test (left) and decomposition during hot needle test (right).

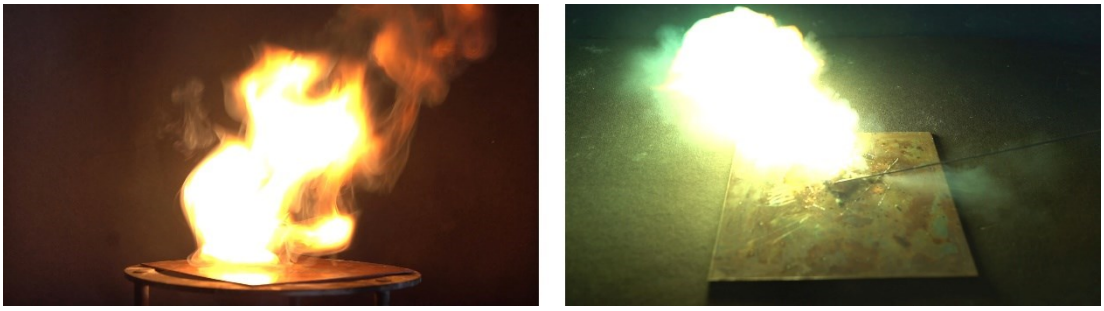

Figure S37. Results of hot plate (left) and hot needle test (right) of compound **18a**.

Figure S38. Results of hot plate (left) and hot needle test (right) of compound **18c**.

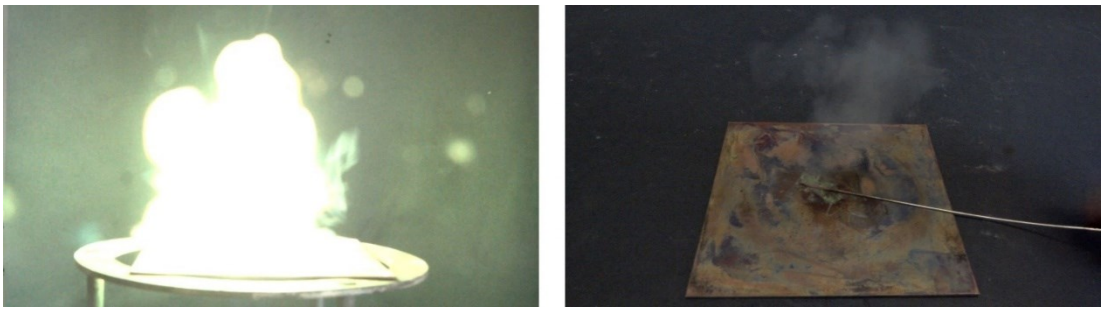

Figure S39. Coordination compound **19** during hot plate (left) and hot needle (right) testings.

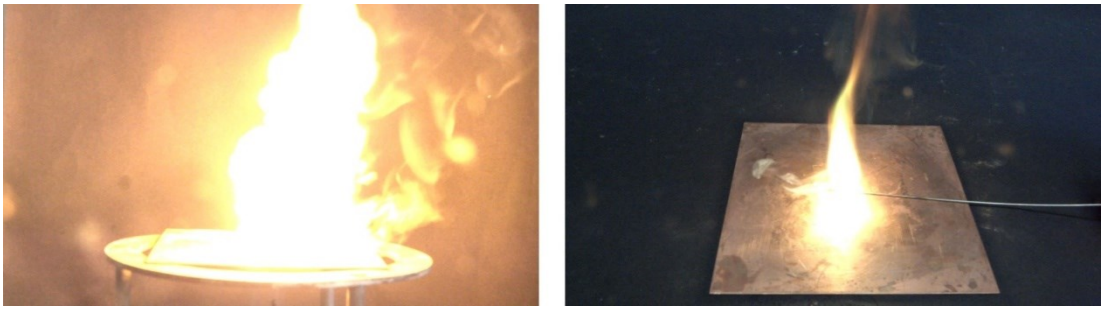

Figure S40. Deflagration of the picrate complex **20** during hot plate test (left) and hot needle tests (right).

Figure S41. Results of hot plate (left) and hot needle test (right) of the styphnate coordination compound **21**.

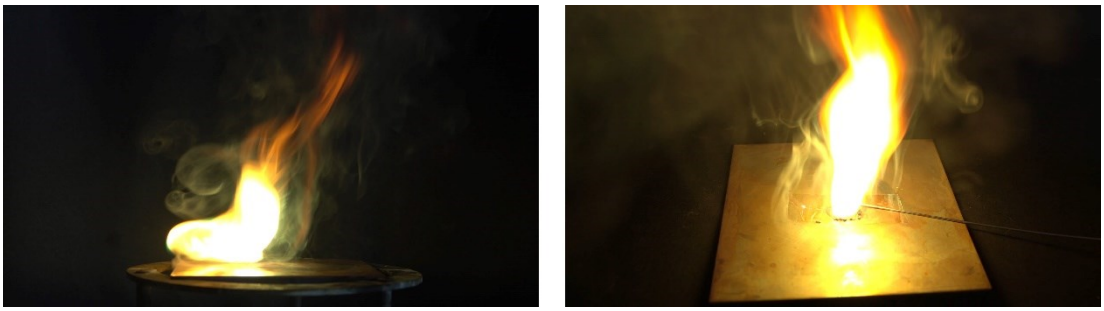

Figure S42. Reactions of ECC **22a** during hot plate (left) and hot needle (right) testings.

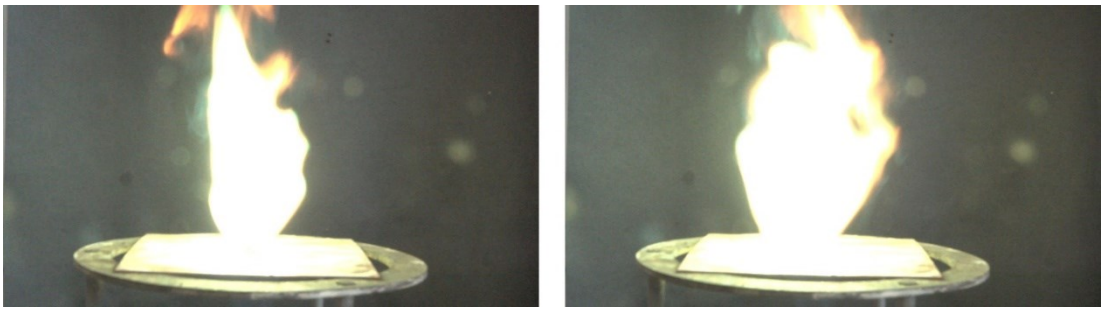

Figure S43. Deflagrations of compound **22b** during hot plate (left) and hot needle tests (right).

Figure S44. Reactions of compound **22c** during hot plate (left) and hot needle tests (right).

8. Experimental Part & General Methods

All chemicals and solvents were employed as received (Sigma-Aldrich, Fluka, Acros, ABCR). ^{1}H, ^{13}C, ^{14}N, and $^{15}N\{^{1}H\}$, and ^{1}H-^{15}N HMBC NMR spectra were recorded at ambient temperature using a JEOL Bruker 27400, Eclipse 270, JEOL EX 400 or a JEOL Eclipse 400 instrument. The chemical shifts quoted in ppm in the text refer to typical standards such as tetramethylsilane (^{1}H, ^{13}C) nitromethane (^{14}N,^{15}N) in DMSO-d_6, acetonitrile-d_3 or acetone-d_6 as the solvent. Endothermic and exothermic events of the described compounds, which indicate melting, loss of crystal water or decomposition, are given as the extrapolated onset temperatures. The samples were measured in a range of 25–400 °C at a heating rate of 5 °C min^{-1} through differential thermal analysis (DTA) with an OZM Research DTA 552-Ex instrument and in some cases additionally by thermal gravimetric analysis (TGA) with a PerkinElmer TGA4000. Infrared spectra were measured with pure samples on a Perkin-Elmer BXII FT-IR system with a Smith DuraSampler IR II diamond ATR. Determination of the carbon, hydrogen, and nitrogen contents was carried out by combustion analysis using an Elementar Vario El (nitrogen values determined are often lower than the calculated ones' due to their explosive behavior). UV-Vis spectra were recorded in the solid state using a Varian Cary 500 spectrometer in the wavelength range of 350–1000 nm. The step in the absorption intensity at 800 nm is caused by a detector change. Impact sensitivity tests were carried out according to STANAG 4489[S23] with a modified instruction[S24] using a BAM (Bundesanstalt für Materialforschung) drophammer.[S25] Ball drop impact sensitivity tests were determined for selected compounds on an OZM ball drop machine (BIT-132), following MIL-STD-1751A (method 1016) by dropping a free-falling steel ball onto the explosive compound.[S26,27] Details on the process can be found in the literature.[S28] Friction sensitivity tests were carried out according to STANAG 4487[S29] with a modified instruction[S30] using the BAM friction tester.[S25,26] The classification of the tested compounds results from the "UN Recommendations on the Transport of Dangerous Goods".[S31,32] Additionally, all compounds were tested upon the sensitivity toward electrical discharge using the OZM Electric Spark XSpark10 device.[S26] Hot plate and hot

needle tests were performed in order to evaluate the potential initiation capability of selected compounds. The samples were fixed on a copper plate underneath adhesive tape and initiated by a red-hot needle. Strong deflagration or detonation of the compound usually indicates a valuable primary explosive. The safe and straightforward hot plate test only shows the behavior of the unconfined sample toward fast heating on a copper plate. It does not necessarily allow any conclusions on a compound's capability as a suitable primary explosive. The laser initiation experiments were performed with a 45 W InGaAs laser diode operating in the single-pulsed mode. The diode is attached to an optical fiber with a core diameter of 400 µm and a cladding diameter of 480 µm. The optical fiber is connected via a SMA type connecter directly to the laser and to a collimator. This collimator is coupled to an optical lens, which was positioned in its focal distance (*f* = 29.9 mm) to the sample. The lens is shielded from the explosive by a sapphire glass. Approximately 15 mg of the carefully pestled compound to be investigated was filled into a transparent plastic cap (PC), pressed with a pressure force of 1 kN and sealed by a UV-curing adhesive. The confined samples were irradiated at a wavelength of 915 nm, a voltage of 4 V, a current of 7 A and pulse lengths of 1–30 ms. The combined currents and pulse lengths result in an energy output of 1.7–51.0 mJ. Energetic properties have been calculated with the EXPLO5 6.05.04 computer code[S33] using the, to RT converted, X-ray density and calculated solid state heats of formation. These were computed by the atomization method as described in recently published papers. Electronic enthalpies were calculated with the Gaussian09 software[S13] suite using the CBS-4M method.

The obtained compounds were washed with acetonitrile when stated, dried overnight in air and used for analytics without further purification.

CAUTION! *All investigated compounds are potentially explosive energetic materials, which show partly increased sensitivities toward various stimuli (e.g. elevated temperatures, impact, friction or electrostatic discharge). Therefore, proper security precautions (safety glass, face shield, earthed equipment and shoes, leather coat, Kevlar gloves, Kevlar sleeves and ear plugs) have to be applied while synthesizing and handling the described compounds.*

2-Aminoethylacetate hydrocloride (1)

2-Aminoethanol hydrocloride (20.0 g, 0.21 mol) was suspended in acetic anhydride (23 g, 0.23 mol).[S33] The reaction mixture was heated to 80 °C for 2 h. The resulting clear solution was cooled to room temperature. The formed parcipitate was filrated off, washed wit diethylether (200 mL) and dried in vacuum over night. Compound **1** was obtained as a colorless solid. Yield: 21.4 g (0.153 mol, 75%).

EA ($C_4H_{10}ClNO_2$, 138.57): calcd: C 34.42, H 7.22, N 10.04%; found: C 34.17, H 7.22, N 10.04%; IR (ATR, cm^{-1}): $\tilde{\nu}$ = 2908 (s), 2895 (s), 2824 (m), 2700 (w), 2646 (w), 2507 (w), 1736 (vs), 1698 (w), 1649 (w), 1622 (w), 1592 (m), 1579 (m), 1524 (s), 1441 (m), 1399 (w), 1380 (m), 1365 (m), 1312 (m), 1293 (m), 1269 (w), 1234 (s), 1137 (w), 1071 (s), 1044 (m), 1031 (s), 985 (s), 890 (s), 868 (w), 799 (m), 651 (m), 607 (m), 436 (m); ^{1}H NMR (400 MHz, DMSO-d_6, 25 °C) δ (ppm) = 8.23 (s, 3H, NH_3), 4.19 (t, $^3J_{H-H}$ = 5.3 Hz, 2H, CH_2), 3.04 (t, $^3J_{H-H}$ = 5.4 Hz, 2H, CH_2), 2.05 (s, 3H, CH_3); ^{13}C NMR (101 MHz, DMSO-d_6, 25 °C) δ (ppm) = 170.3, 60.4, 37.8, 20.7; HRMS (ESI) for $C_4H_{10}ClNO_2$ calc. $[M–Cl]^+$ 104.0706, found: 104.0707.

2-(1*H*-tetrazol-1-yl)ethyl acetate (2)

Compound **1** (21.4 g, 0.15 mol) and sodium azide (11.9 g, 0.18 mol) were suspended in trietylorthoformiate (91.0 g, 102.1 mL, 0.61 mol).[S34] Acetic acid (61 mL) was added dropwise

under stirring over a period of 30 min. The suspension was heated to reflux for 3 h. After cooling to RT, the solvent was removed under reduced pressure and the remaining solid was extracted with hot acetone (200 mL). The solvent was evaporated and theremaining colorless oil was dried under high vacuum. The compound solidified yielding 2-(1*H*-tetrazol-1-yl)ethyl acetate (**2**) as colorless block suitable for single crystal X-ray diffraction. Yield: 14.6 g (0.094 mol, 61%).

EA ($C_5H_8N_4O_2$, 156.15): calcd: C 38.46, H 5.16, N 35.88%; found: C 38.27, H 4.90, N 35.82%; IR (ATR, cm^{-1}): $\tilde{\nu}$ = 2979 (vw), 1731 (s), 1694 (w), 1660 (w), 1483 (m), 1473 (m), 1459 (w), 1444 (w), 1431 (m), 1389 (m), 1376 (m), 1359 (m), 1279 (m), 1267 (m), 1249 (s), 1229 (vs), 1174 (s), 1103 (s), 1080 (s), 1049 (s), 1025 (s), 995 (m), 978 (m), 962 (m), 940 (s), 881 (s), 833 (m), 723 (w), 677 (s), 651 (s), 639 (m), 602 (m), 502 (s), 429 (m); ^{1}H NMR (400 MHz, DMSO-d_6, 25 °C) δ (ppm) = 9.44 (s, 1H, CH), 4.75 (t, $^3J_{H-H}$ = 5.2 Hz, 1H, CH_2), 4.53–4.27 (m, 2H, CH_2), 1.98 (s, 3H,CH_3); ^{13}C NMR (101 MHz, DMSO-d_6, 25 °C) δ (ppm) = 170.0, 144.3, 61.6, 46.8, 20.4; HRMS (EI) for $C_5H_8N_4O_2$ calc. $[M+H]^+$ 157.0720, found: 157.0714.

1-Hydroxyethyl-5*H*-tetrazole (3)

Compound **2** (14.0 g, 0.09 mmol) was dissolved in concentrated hydrochloric acid (10 mL) and stirred at room temperature for 1 h. The solvent was removed under reduced pressure and the resulting colorless oil was dried under high vaccum. The oil solidified yielding compound **3** in the form of colorless blocks. Yield: 8.9 g (0.078 mmol, 87%).

^{1}H NMR (400 MHz, DMSO-d_6, 25 °C) δ (ppm) = 9.33 (s, 1H, CH), 5.11 (s, 2H, OH), 4.50 (t, $^3J_{H-H}$ = 5.3 Hz, 4H, CH_2), 3.78 (t, $^3J_{H-H}$ = 5.3 Hz, 4H, CH_2); ^{13}C NMR (101 MHz, DMSO-d_6, 25 °C) δ (ppm) = 144.3, 59.1, 50.4; HRMS (EI) for $C_3H_6N_4O$ calc. [M] 114.0542, found: 114.0542.

One-pot synthesis of 1-Hydroxyethyl-5*H*-tetrazole (3)

2-Aminoethanol hydrochloride (19.5 g, 0.20 mol) was suspended in acetic anhydride (22.5 g, 0.22 mol) in a 500 mL three necked roundbottom flask. The reaction mixture was heated to 80 °C for 2 hours. Subsequently the solution was allowed to cool down to 40 °C and triethylorthoformiate (59.3 g, 66.3 mL, 0.40 mol) was added. Sodium azide (15.6 g, 0.24 mol) was added and acetic acid (70 mL) was added dropwise. After the complete addition, the reaction mixture was refulxed for 3 h. Afterwards concentrated hydrochloric acid (40 mL) was added and heating was continued for 30 min. The solution was cooled to RT and the solvent was removed. The remaining suspension was extracted with hot acetone (200 mL) and the solvent was removed *in vacuo*. The remaining colorless oil was dried under high vaccum and solidified. Compound **3** was obatined in the form of colorless blocks. Yield: 17.1 g (0.15 mol, 75%).

Selective preparation of 1-nitratoethyltetrazole (1-NET, 4)

White fuming nitric acid (12 mL) was cooled to 0 °C and compound **3** (2.0 g, 17.5 mmol) was added dropwise. The temperature was kept below 10 °C during the whole addition. Stirring was continued for 20 min. Subsequently the solution was allowed to warm to room temperature and stirred mechanical for another 20 min. After neutralization using sodium carbonate, the aqueous layer was extracted with dichloromethane (3x, 200 mL). The combined organic layers were dried over magnesium sulfate and the solvent was removed under reduced pressure. The remaining cololess oil was dried under high vaccum and solidified. The tetrazole derivative **4** was obtained in the form of colorless blocks suitable for single crystal X-ray diffraction. Yield: 2.0 g (12.8 mmol, 73%).

Preparation of 1- & 2-nitratoethyltetrazole via alkylation of 1,5*H*-tetrazole (1-NET, 4; 2-NET, 5)

1,5*H*-tetrazole (7.0 g, 0.10 mol) was suspended in water (15 mL).[S35] Sodium hydroxide (4.0 g, 0.10 mol) dissolved in water (15 mL) was added and the solution was heated to reflux. 2-Chloroethanol (10.1 g, 8.3 mL, 0.13 mmol) was added dropwise over the course of 15 min. The reaction mixture was heated to reflux for 12 h. The solvent was removed under reduced pressure and the resulting suspension was extracted with hot acetone (600 mL). Removal of the solvent *in vacuo* afforded a mixture of 1- and 2-hydroxy-5*H*-ethyltetrazole as a yellowish oil in almost quantitative yield (11.2 g, 0.098 mol, 98%). The isomers were not seperated.

^{1}H NMR (400 MHz, DMSO-d_6, 25 °C) δ (ppm) = 9.34 (s, 1H, CH), 8.95 (s, 1H, CH), 5.18–4.97 (m, 2H, OH), 4.76–4.66 (m, 2H, CH_2), 4.58– 4.43 (m, 2H, CH_2), 3.90 (t, $^{3}J_{H-H}$ = 5.3 Hz, 3H, CH_2), 3.78 (t, $^{3}J_{H-H}$ = 5.2 Hz, 3H, CH_2); ^{13}C NMR (101 MHz, DMSO-d_6, 25 °C) δ (ppm) = 50.4, 55.4, 59.1, 59.1, 144.3, 153.2.

Subsequently white fuming nitric acid (12 mL) was cooled to 0 °C. The mixture of both tetrazole derivatives (2.1 g, 18.40 mmol) was added dropwise whereas the temperature was kept below 10 °C during the whole addition. After stirring for 20 min the mixture was allowed to warm to RT and stirring was continued for a further 20 min. Sodium carbonate was added until a pH-level of 7. The remaining solution was extracted with dichloromethane (3x, 200 mL). The combined organic layers were dried over magnesium sulfate and the solvent was evaporated under reduced pressure. Purification via flash column chromatography (1:1 ethyl acetate/*i*haxane → pure ethyl acetate) afforded 1-nitratoethyl-5*H*-tetrazole (**4**, 1.31 g, 7.98 mmol, 45%) and 2-nitratoethyltetrazole (**5**, 1.27 g, 8.23 mmol, 43%) as colorless oils. Subjecting the samples to high vacuum led to their solidification, leading to colorless block suitable for X-ray diffraction in case of compound **4**. Single crystals of compound **5** could be achieved through sublimation (40 °C, 0.5 x 10^{-2} mbar).

1-NET (4)

EA ($C_3H_5N_5O_3$, 159.11): calcd: C 22.65, H 3.17, N 44.02%; found: C 22.55, H 3.23, N 43.31%; IR (ATR, cm^{-1}): $\tilde{\nu}$ = 3010 (w), 2967 (w), 2900 (w), 1763 (w), 1641 (s), 1620 (s), 1526 (w), 1485 (m), 1460 (m), 1434 (m), 1427 (m), 1393 (m), 1369 (m), 1282 (vs), 1238 (m), 1172 (s), 1111 (s), 1076 (w), 1019 (s), 978 (m), 966 (m), 897 (vs), 885 (s), 861 (s), 760 (s), 711 (vs), 681 (s), 651 (s), 567 (s), 486 (m); ^{1}H NMR (400 MHz, DMSO-d_6, 25 °C) δ (ppm) = 9.46 (s, 1H, CH), 4.99–495 (m, 2H, CH_2), 4.93–4.88 (m, 2H, CH_2); ^{13}C NMR (101 MHz, DMSO-d_6, 25 °C) δ (ppm) = 144.4, 70.8, 45.2; ^{14}N NMR (29 MHz, DMSO-d_6, 25 °C) δ (ppm) = –43.5; HRMS (ESI) for $C_3H_5N_5O_3$ calc. $[M+H]^+$ 160.0465, found: 160.0467; BAM drophammer: 10 J, BAM friction tester: > 360 N (at grain size ≈ 500–1000 µm).

2-NET (5)

EA ($C_3H_5N_5O_3$, 159.11): calcd: C 22.65, H 3.17, N 44.02%; found: C 22.94, H 2.87, N 43.83%; IR (ATR, cm^{-1}): $\tilde{\nu}$ = 3033 (vw), 2976 (vw), 2914 (vw), 1768 (vw), 1643 (s), 1632 (s), 1514 (vw), 1456 (w), 1451 (w), 1429 (m), 1380 (w), 1365 (w), 1352 (m), 1335 (w), 1324 (w), 1277 (vs), 1240 (m), 1192 (m), 1162 (m), 1134 (m), 1067 (m), 1035 (s), 1025 (m), 1013 (m), 987 (m), 923 (w), 886 (s), 850 (s), 755 (s), 714 (m), 708 (m), 697 (s), 671 (s), 570 (m), 487 (m); ^{1}H NMR (400 MHz, DMSO-d_6, 25 °C) δ (ppm) = 9.04 (s, 1H, CH), 5.19–5.12 (m, 2H, CH_2), 5.08–5.01 (m, 2H, CH_2); ^{13}C NMR (101 MHz, DMSO-d_6, 25 °C) δ (ppm) = 153.6, 70.4, 50.1; ^{14}N NMR (29 MHz, DMSO-d_6, 25 °C) δ (ppm) = –43.0; ^{15}N NMR (41 MHz, Acetone-d_6, 25 °C) δ (ppm) = –0.7 (s), –44.5 (t), –46 .1(d), –76.1 (d), 100.9 (m); HRMS (ESI) for $C_3H_5N_5O_3$ calc. $[M+H]^+$ 160.0465, found: 160.0462; BAM drophammer: 2 J, BAM friction tester: > 360 N (at grain size ≈ 500–1000 µm).

[Cu(1-NET)$_3$(NO$_3$)$_2$] (6)

Copper nitrate trihydrate (60.4 mg, 0.25 mmol) was dissolved in accetonitrile (2 mL). Compound **4** was added in stochiometric amounts in acetonitrile (2 mL). Complex **6** was obtained in the form of blue platelets suitable for X-ray diffraction within a days. Yield: 133.0 mg (0.20 mmol, 81%).

DTA (5 °C min^{-1}) onset: 121 °C (endothermic), 169 °C (exothermic); IR (ATR, cm^{-1}): $\tilde{\nu}$ = 3038 (w), 2987 (vw), 2898 (vw), 1817 (vw), 1731 (vw), 1659 (w), 1625 (s), 1508 (m), 1469 (s), 1449 (m), 1431 (s), 1382 (w), 1364 (m), 1315 (s), 1289 (s), 1273 (vs), 1188 (m), 1167 (m), 1104 (m), 1088 (m), 1015 (s), 997 (s), 942 (w), 911 (m), 902 (m), 881 (s), 846 (s), 808 (s), 759 (m), 726 (w), 714 (w), 697 (m), 662 (s), 643 (m), 575 (m), 492 (m), 449 (vw); EA ($C_9H_{15}CuN_7O_{15}$, 664.86): calcd: C 16.26, H 2.27, N 35.81%; found: C 16.85, H 2.21, N 35.93%; BAM drophammer: 5 J; BDIS: 14 mJ, BAM friction tester: 48 N; ESD: 1080 mJ (at grain size ≈ 500–1000 µm).

[Cu(DN)$_2$(1-NET)$_2$] (7)

Dinitraminic acid was prepared according to our previously published method.[S36] Basic copper(II) carbonate (55.3 mg, 0.25 mmol) was dissolved in dinitraminic acid (4 mL). Compound **4** was added in stochiometric amounts. Complex **7** was obtained in the form of blue needle suitable for X-ray diffraction within five days. Yield: 143 mg (0.24 mmol, 96%).

DTA (5 °C min^{-1}) onset: 110 °C (exothermic); IR (ATR, cm^{-1}): $\tilde{\nu}$ = 3018 (w), 2976 (vw), 2906 (vw), 1651 (s), 1628 (s), 1571 (vs), 1513 (s), 1460 (m), 1432 (m), 1389 (w), 1375 (w), 1365 (w), 1322 (m), 1297 (w), 1279 (vs), 1243 (w), 1213 (s), 1202 (s), 1182 (vs), 1109 (s), 1075 (w), 1036 (s), 1000 (vs), 891 (vs), 854 (s), 828 (s), 755 (s), 743 (vs), 710 (s), 685 (s), 653 (s), 571 (m), 487 (m), 477 (w), 458

(m); EA ($C_6H_{10}CuN_{16}O_{14}$, 593.79): calcd: C 12.14, H 1.70, N 37.74%; found: C 12.08, H 1.72, N 37.32%; BAM drophammer: 2 J; BDIS: 14 mJ, BAM friction tester: 7 N; ESD: 1080 mJ (at grain size ≈ 500–1000 µm).

General method for the preparation of ECC 8 & 9

Copper(II) chlorate or Zinc(II) chlorate were prepared according to a literature known method.[S37] Copper sulfate pentahydrate (62.4 mg, 0.25 mmol) or zinc sulfate heptahydrate (71.9 mg, 0.25 mmol) was dissolved in water (2 mL) and barium chlorate monohydrate (76.1 mg, 0.25 mmol) in water (4 mL) was added. Stirring was continued for 5 min and the solution was filtrated using a syringe filter. The solvent was removed under reduced pressure and acetonitrile was added. Stochiometric amounts of ligand **4** dissolved in acetonitrile (2 mL) were added and the solution was left for crystalization.

$[Cu(1\text{-}NET)_6](ClO_3)_2$ (8)

Blue platelets of complex **8** suitable for single crystal X-ray diffraction were obtained within a week. Yield: 249 mg (0.21 mmol, 84%).

DTA (5 °C min^{-1}) onset: 54 °C (endothermic), 149 °C (exothermic); IR (ATR, cm^{-1}): $\tilde{\nu}$ = 3104 (w), 3035 (vw), 2978 (vw), 2905 (vw), 1743 (vw), 1629 (vs), 1507 (m), 1451 (w), 1443 (w), 1389 (vw), 1367 (w), 1276 (vs), 1181 (m), 1109 (s), 1077 (w), 1065 (w), 1037 (m), 1008 (m), 961 (vs), 933 (s), 887 (vs), 847 (vs), 756 (m), 708 (m), 690 (m), 679 (m), 650 (s), 634 (m), 604 (m), 567 (m), 487 (m), 478 (s); EA ($C_{18}H_{30}CuN_{30}O_{24}$): calcd: C 18.24, H 2.55, N 35.46%; found: C 18.51, H 2.45, N 35.25%;

BAM drophammer: 2 J; BDIS: 55 mJ, BAM friction tester: 15 N; ESD: 250 mJ (at grain size ≈ 500–1000 µm).

$[Zn(1\text{-}NET)_6](ClO_3)_2$ (9)

Colorless platelets of complex **9** suitable X-ray diffraction were obtained within a week. Yield: 237 mg (0.20 mmol, 80%).

DTA (5 °C min^{-1}) onset: 71 °C (endothermic), 154 °C (exothermic); IR (ATR, cm^{-1}): $\tilde{\nu}$ = 3020 (vw), 2979 (vw), 2904 (vw), 1643 (s), 1626 (vs), 1505 (m), 1453 (m), 1435 (w), 1390 (w), 1370 (w), 1278 (vs), 1178 (m), 1108 (s), 1079 (w), 1035 (m), 1004 (s), 961 (vs), 934 (s), 886 (vs), 844 (vs), 756 (m), 721 (w), 705 (m), 684 (m), 649 (s), 604 (m), 565 (m), 493 (m), 477 (s); EA ($C_{18}H_{30}Cl_2CuN_{30}O_{24}$): calcd: C 18.22, H 2.55, N 35.40%; found: C 18.36, H 2.60, N 35.30%; BAM drophammer: 7 J; BDIS: 69 mJ, BAM friction tester: 14 N; ESD: 750 mJ (at grain size ≈ 500–1000 µm).

General method for the preparation of ECC 10–13

The respective metal perchlorate (**10**: $Mn(ClO_4)_2 \cdot 6\ H_2O$ (90.5 mg, 0.25 mmol); **11**, **13**: $Cu(ClO_4)_2 \cdot 6\ H_2O$ (92.6 mg, 0.25 mmol); 12: $Zn(ClO_4)_2 \cdot 6\ H_2O$ (93.1 mg, 0.25 mmol)) was dissolved in acetonitrile (2 mL). For the preparation of the complexes **10**–**12** stochiometric amounts of ligand **4** were dissolved in acetonitrile (2 mL) and added. To obtain complex **13**, ligand **5** in acetonitrile (2 mL) was added instead of ligand **4**. The mixture was stirred for 5 min at ambient temperature. Subsequently the solution was left for crystalization.

$[Mn(1\text{-}NET)_6](ClO_4)_2$ (10)

Single crystals in the form of colorless blocks of compound **10** were obtained within two weeks. Due to the low melting point of the complex, it was not possible to isolate the compound on a large scale.

$[Cu(1\text{-}NET)_6](ClO_4)_2$ (11)

Blue blocks of compound **11** suitable for X-ray diffraction were obtained within two days. Yield: 231.2 mg (0.19 mmol, 76%).

DTA (5 °C min^{-1}) onset: 70, 117 °C (endothermic), 165 °C (exothermic); IR (ATR, cm^{-1}): $\tilde{\nu}$ = 3049 (vw), 3021 (vw), 2978 (vw), 2904 (vw), 1642 (s), 1631 (s), 1541 (vw), 1509 (m), 1496 (w), 1453 (w), 1429 (m), 1388 (w), 1369 (w), 1323 (w), 1280 (vs), 1243 (w), 1185 (m), 1175 (m), 1106 (s), 1082 (vs), 1046 (m), 1030 (s), 1000 (s), 961 (m), 934 (w), 882 (s), 839 (vs), 753 (m), 723 (w), 698 (m), 686 (m), 653 (s), 622 (vs), 565 (w), 544 (vw), 522 (w), 486(m); EA ($C_{18}H_{30}Cl_2CuN_{30}O_{26}$): calcd: C 17.76, H 2.48, N 34.53%; found: C 17.62, H 2.45, N 34.29%; BAM drophammer: 3 J; BDIS: > 200 mJ, BAM friction tester: 25 N; ESD: 480 mJ (at grain size < 100 µm).

$[Zn(1\text{-}NET)_6](ClO_4)_2$ (12)

Colorless blocks of compound **12** suitable for structure determination were obtained within two weeks. Due to the low melting point of the coordination compound, it was not possible to isolate the ECC on a large scale.

$[Cu(2\text{-}NET)_6](ClO_4)_2$ (13)

Blue blocks of compound **13** were obtained within a week. Yield: 270 mg (0.22 mmol, 89%).

DTA (5 °C min^{-1}) onset: 65 °C (endothermic), 143 °C (exothermic); IR (ATR, cm^{-1}): $\tilde{\nu}$ = 3036 (vw), 3027 (vw), 2977 (vw), 2905 (vw), 1742 (vw), 1631 (vs), 1554 (w), 1459 (w), 1434 (w), 1387 (w), 1365 (w), 1345 (vw), 1308 (w), 1278 (vs), 1248 (w), 1203 (w), 1189 (w), 1144 (m), 1096 (s), 1082 (vs), 1050 (s), 1035 (s), 1027 (s), 985 (m), 932 (w), 890 (vs), 850 (vs), 756 (s), 707 (m), 689 (s), 677 (s), 621 (vs), 570 (m), 516 (m), 508 (m), 490 (m), 463 (w); EA ($C_{18}H_{30}Cl_2CuN_{30}O_{26}$): calcd: C 17.76, H 2.48, N 34.53%; found: C 17.38, H 2.49, N 33.20%; BAM drophammer: 2 J; BDIS: 55 mJ, BAM friction tester: 5 N; ESD: 1080 mJ (at grain size ≈ 100–500 µm).

General method for the preparation of single crystals of ECC 14 & 15

Sodium azide (32.5 mg, 0.50 mmol) and the respective ligand **4** or **5** (238.7 mg, 1.5 mmol) were dissolved in water (6 mL). The solution was carefully layerd with a 1:1 mixture of ethanol (4 mL) followed by copper(II) chloride dihydrate (42.6 mg, 0.25 mmol) dissolved in ethanol (6 mL).[S38]

$[Cu(N_3)_2(1\text{-}NET)]$ (14)

Copper(II) sulfate pentahydrate (62.4 mg, 0.25 mmol) was dissolved in water (4 mL) and stochiometric amounts of ligand **4** were added.[S38] The solution was heated to 60 °C until the complete dissolution of the ligand. Sodium azide (32.5 mg, 0.50 mmol) dissolved in water (2 mL) was added dropwise ofer a period of 5 min. Stirring was continued for 15 min. The formed brown parcipitate was filtrated off and washed with water (20 mL). Coordination compound **14** was obtained as a brown solid. Yield: 64.4 mg (0.21 mmol, 82%).

Single crystals in the form of brown platelets acoording to the general procedure were obtained within a week.

DTA (5 °C min^{-1}) onset: 122 °C (exothermic); IR (ATR, cm^{-1}): $\tilde{\nu}$ = 3110 (w), 3024 (vw), 2094 (s), 2076 (s), 2050 (vs), 2041 (vs), 1976 (w), 1752 (vw), 1642 (s), 1506 (m), 1450 (w), 1432 (m), 1385 (vw), 1371 (w), 1343 (vw), 1279 (s), 1234 (w), 1181 (m), 1104 (m), 1079 (m), 1061 (w), 1050 (w), 1030 (w), 1015 (m), 992 (m), 903 (w), 887 (s), 846 (s), 753 (m), 718 (vw), 692 (m), 659 (s), 637 (w), 601 (m), 595 (w), 585 (w), 572 (w), 485 (w), 416 (w), 410 (w); EA ($C_3H_5CuN_{11}O_3$): calcd: C 11.75, H 1.64, N 50.24%; found: C 12.04, H 1.84, N 49.26%; BAM drophammer: 4 J; BDIS: ≤ 4 mJ, BAM friction tester: 1 N; ESD: 14 mJ (at grain size < 100 µm).

$[Cu_2(N_3)_4(2\text{-NET})]$ (15)

Brown platelets of ECC **15** were obtained within two weeks according to the general procedure. An elemental analysis pure isolation of the coordination compound was not possible.

$[Ag_2(CNO)_2(1\text{-NET})]$ (16a)

Complex **16a** was prepared according to a recently published procedure.[S39] Silver fulminate (37.5 mg, 0.25 mmol)was dissolved in a mixture of water (2 mL) and acetonitrile (2 mL) at 60 °C. Ligand **4** (159.1 mg,) dissolved in acetonitrile (2 mL) were added and stirring was continued for 5 min. Collorless needles of **16a** suitbale for X-ray diffraction were isolated within two days. Yield: 49.0 mg (0.11 mmol, 43%).

DTA (5 °C min^{-1}) onset: 96 °C (endothermic), 123 °C (exothermic); IR (ATR, cm^{-1}): $\tilde{\nu}$ = 3032 (vw), 2970 (vw), 2905 (vw), 2311 (w), 2295 (w), 2248 (m), 2106 (s), 2089 (vs), 1641 (s), 1634 (s), 1595 (m), 1558 (m), 1494 (m), 1447 (m), 1436 (m), 1330 (w), 1313 (w), 1279 (vs), 1218 (vw), 1173 (m), 1155 (vs), 1127 (s), 1105 (s), 1058 (m), 983 (s), 901 (m), 887 (m), 853 (vs), 763 (m), 753 (s), 718 (m), 708 (w), 687 (w), 681 (w), 659 (s), 605 (m), 578 (w), 503 (w), 483 (m), 464 (m); EA ($C_5H_5Ag_2N_7O_5$, 459.88): calcd: C 13.09, H 1.10, N 21.37%; found: C 13.20, H 1.03, N 21.28%; BAM drophammer: ≤ 1 J; BDIS: 8 mJ, BAM friction tester: 20 N; ESD: 250 mJ (at grain size > 1000 µm).

[Ag(CNO)(1-NET)] (16b)

Complex **16b** was formed by leaving the silver fulminate complex 16a for four weaks in a closed vessel in its mother liqour. Yield: 64.8 mg (0.21 mmol, 84%).

DTA (5 °C min^{-1}) onset: 67 °C (endothermic), 102 °C (endothermic followed by exothermic); IR (ATR, cm^{-1}): $\tilde{\nu}$ = 3139 (m), 3019 (w), 2976 (w), 2905 (w), 2303 (w), 2096 (m), 2066 (m), 1640 (s), 1635 (s), 1627 (s), 1487 (m), 1436 (w), 1417 (m), 1365 (w), 1322 (w), 1316 (w), 1280 (vs), 1180 (m), 1152 (s), 1109 (s), 1081 (m), 1034 (m), 1001 (s), 979 (m), 967 (m), 887 (vs), 878 (s), 849 (vs), 752 (s), 722 (w), 687 (s), 660 (s), 631 (m), 580 (m), 478 (m); EA ($C_4H_5AgN_6O_4$, 308.99): calcd: C 15.55, H 1.63, N 27.20%; found: C 15.57, H 1.62, N 27.31%; BAM drophammer: 9 J; BDIS: 83 mJ, BAM friction tester: 60 N; ESD: 250 mJ (at grain size 100–500 µm).

General procedure for the preparation of the coordination componds 17–19

The preparation of the ECC **17–19** was performed according to our previous work.[S40] Basic copper(II) carbonate (0.25 mmol) was reacted with the corresponding trinitrobenzene derivative based acid (**17**: 115 mg, 0.50 mmol; **18a**: 122.6 mg, 0.50 mmol; **18b**: 61.3 mg, 0.25 mmol; **19**: 131 mg, 0.50 mmol) in water (4 mL) at 80 °C. After the complete dissolution of both compounds, ligand **4** was added in stochiometric amounts. Mechanical stirring was continued for 5 min. Subsequently the solution was left for crystalization at ambient temperature.

$[Cu(1\text{-}NET)_2(PA)_2]$ (17)

Single crystals in the form of green platelets of the picrate complex **17** were obtained after two days 360.3 mg (0.43 mmol, 86%).

DTA (5 °C min^{-1}) onset: 197 °C (exothermic); IR (ATR, cm^{-1}): $\tilde{\nu}$ = 3088 (w), 3036 (w), 1656 (m), 1629 (m), 1607 (s), 1574 (s), 1526 (vs), 1506 (s), 1454 (m), 1427 (m), 1419 (m), 1390 (w), 1360 (m), 1338 (s), 1276 (vs), 1166 (s), 1100 (s), 1086 (s), 1037 (m), 1025 (m), 1006 (m), 956 (w), 936 (m), 915 (m), 905 (m), 895 (m), 884 (s), 845 (s), 785 (m), 760 (w), 742 (m), 715 (s), 707 (s), 688 (s), 659 (s), 634 (m), 574 (w), 552 (m), 523 (m), 486 (w), 462 (w), 428 (vw); EA ($C_{18}H_{14}CuN_{16}O_{20}$, 837.95): calcd: C 25.80, H 1.68, N 26.75%; found: C 25.85, H 1.50, N 26.65%; BAM drophammer: 20 J; BDIS: > 200 mJ, BAM friction tester: > 360 N; ESD: 480 mJ (at grain size < 100 µm).

$[Cu(1\text{-}NET)_2(TNR)]$ (18a)

Compound **18a** was obtained as dark green blocks suitable for X-ray diffraction within a day. Yield: 250.5 mg (0,40 mmol, 80%).

DTA (5 °C min^{-1}) onset: 195 °C (exothermic); IR (ATR, cm^{-1}): $\tilde{\nu}$ = 2910 (w), 1751 (w), 1636 (m), 1618 (w), 1584 (s), 1543 (m), 1524 (s), 1484 (m), 1471 (m), 1429 (s), 1385 (m), 1367 (m), 1344 (w), 1294 (s), 1276 (vs), 1244 (s), 1232 (s), 1172 (m), 1142 (m), 1100 (s), 1066 (w), 1034 (m), 1016 (m), 959 (w), 944 (w), 898 (m), 880 (m), 847 (s), 791 (m), 775 (m), 755 (m), 708 (vs), 690 (m), 682 (m), 650 (m), 570 (w), 492 (w), 473 (w), 433 (w), 423 (m), 418 (m); EA ($C_{12}H_{11}CuN_{13}O_{14}$, 624.84): calcd: C 23.07, H 1.77, N 29.14%; found: C 23.30, H 1.658, N 29.90%; BAM drophammer: 2 J; BDIS: 111 mJ, BAM friction tester: 96 N; ESD: 480 mJ (at grain size < 100 µm).

$[Cu(HTNR)_2(1\text{-}NET)_2] \bullet 2\ H_2O$ (18b)

Single crystals in the form of green blocks of compound **18b** were obtained after one day when recrystallizing complex **18a** in hot water. An elemental analysis pure isolation of the coordination compound was not possible.

$[Cu(HTNR)_2(1\text{-}NET)_4]$ (18c)

Compound **18c** was obtained as green blocks suitable for X-ray diffraction within a day. Yield: 332.7 mg (0.28 mmol, 56%).

DTA (5 °C min^{-1}) onset: 167 °C (exothermic); IR (ATR, cm^{-1}): $\tilde{\nu}$ = 3142 (w), 1641 (s), 1627 (s), 1558 (m), 1537 (s), 1533 (s), 1479 (m), 1456 (m), 1436 (m), 1373 (m), 1353 (m), 1312 (s), 1279 (vs), 1242 (m), 1170 (s), 1090 (s), 1030 (m), 1008 (m), 989 (m), 928 (m), 909 (w), 890 (m), 877 (m), 844 (m), 784 (w), 759 (w), 735 (m), 715 (m), 696 (s), 679 (s), 657 (m), 568 (w); EA ($C_{24}H_{24}CuN_{26}O_{28}$, 1188.16): calcd: C 24.26, H 2.04, N 30.65%; found: C 24.43, H 1.79, N 25.40%; BAM drophammer: 5 J; BDIS: > 200 mJ, BAM friction tester: 96 N; ESD: >1500 mJ (at grain size ≈ 500–1000 µm).

[Cu(H_2TNPG)$_2$(1-NET)$_4$] (19)

After two days single crystals in the form of green blocks of ECC **19** were obtained. Yield 414.9 mg (0.34 mmol, 68%).

DTA (5 °C min^{-1}) onset: 169 °C (exothermic); IR (ATR, cm^{-1}): $\tilde{\nu}$ = 3024 (w), 2979 (w), 2907 (w), 1635 (vs), 1568 (m), 1505 (s), 1497 (s), 1454 (m), 1426 (m), 1394 (w), 1333 (s), 1277 (vs), 1233 (w), 1179 (s), 1155 (s), 1136 (s), 1099 (s), 1043 (m), 1030 (s), 1007 (s), 914 (m), 892 (s), 851 (s), 835 (s), 814 (s), 785 (s), 758 (s), 731 (s), 708 (s), 693 (s), 678 (s), 649 (s), 632 (s), 625 (s), 568 (m), 538 (w), 519 (w), 505 (w), 490 (m), 458 (w); EA ($C_3H_5CuN_{11}O_3$, 1220.15): calcd: C 23.63, H 1.98, N 29.85%; found: C 23.75, H 1.94, N 29.72%; BAM drophammer: 2 J; BDIS: > 200 mJ, BAM friction tester: 96 N; ESD: 1080 mJ (at grain size ≈ 500–1000 µm).

General procedure for the preparation of the coordination componds 20–22

The coordination compounds **20**–**22** were prepared according to our previous work.[S40] Basic copper(II) carbonate (0.25 mmol) was reacted with the corresponding trinitrobenzene derivative based acid (**20**: 115 mg, 0.50 mmol; **21**: 61.3 mg, 0.25 mmol; **22a**: 65.3 mg, 0.25 mmol; **22b–c**: 131 mg, 0.50 mmol) in water (4 mL) at 80 °C. After the complete dissolution of both compounds, ligand **5** was added in stochiometric amounts. Mechanical stirring was continued for 5 min. Subsequently the solution was left for crystalization at ambient temperature.

[Cu(2-NET)$_2$(PA)$_2$] (20)

Single crystals in the form of green platelets of the picrate complex **20** were obtained after two days. Yield: 310.0 mg (0.37 mmol, 74%).

DTA (5 °C min^{-1}) onset: 165 °C (endothermic followed by exothermic); IR (ATR, cm^{-1}): $\tilde{\nu}$ = 3101 (w), 3022 (w), 2987 (w), 2972 (w), 2914 (w), 2850 (vw), 1633 (vs), 1611 (s), 1579 (vs), 1538 (vs), 1510 (vs), 1475 (m), 1471 (m), 1438 (m), 1430 (m), 1417 (m), 1402 (w), 1390 (w), 1364 (s), 1337 (vs), 1309 (s), 1283 (vs), 1267 (vs), 1251 (vs), 1198 (s), 1167 (s), 1141 (vs), 1102 (m), 1085 (s), 1059 (m), 1036 (m), 1003 (s), 970 (m), 947 (m), 933 (w), 922 (m), 916 (m), 901 (m), 890 (s), 843 (s), 827 (s), 788 (s), 752 (m), 744 (s), 723 (s), 714 (s), 706 (s), 693 (s), 676 (s), 637 (m), 571 (m), 554 (m), 536 (m), 510 (s), 442 (m); EA ($C_{18}H_{14}CuN_{16}O_{20}$, 837.95): calcd: C 25.80, H 1.68, N 26.75%; found: C 25.85, H 1.75, N 26.94%; BAM drophammer: 3 J; BDIS: > 200 mJ, BAM friction tester: 192 N; ESD: 1080 mJ (at grain size ≈ 500–1000 µm).

[Cu(2-NET)$_2$(TNR)] (21)

The syphnate complex **21** was obtained as green plates suitable for X-ray diffraction in four days. Yield: 249.9 mg (0.40 mmol, 80%).

DTA (5 °C min^{-1}) onset: 161 °C (exothermic); IR (ATR, cm^{-1}): $\tilde{\nu}$ = 3156 (w), 3103 (vw), 3033 (vw), 2971 (vw), 2921 (vw), 2889 (vw), 1647 (m), 1623 (m), 1586 (s), 1543 (s), 1527 (s), 1481 (m), 1468 (s), 1436 (s), 1378 (s), 1363 (m), 1310 (m), 1292 (s), 1274 (vs), 1243 (s), 1228 (s), 1213 (s), 1195 (s), 1171 (s), 1155 (m), 1142 (s), 1105 (s), 1053 (m), 1034 (m), 1018 (m), 1012 (m), 985 (m), 966 (w), 930 (w), 904 (m), 884 (s), 860 (m), 844 (s), 789 (w), 775 (m), 755 (m), 733 (w), 706 (s), 699 (vs), 676 (s), 667 (m), 645 (m), 590 (w), 574 (m), 513 (m), 466 (w), 422 (m); EA ($C_{12}H_{11}CuN_{13}O_{14}$, 624.84): calcd: C 23.07, H 1.77, N 29.14%; found: C 23.06, H 1.73, N 29.04%; BAM drophammer: ≤ 1 J; BDIS: 138 mJ, BAM friction tester: 80 N; ESD: 750 mJ (at grain size < 100 µm).

[Cu(HTNPG)(2-NET)$_2$] (22a)

Dark green blocks from compound **22a** suitable for crystal structure determination were obtained within ten days. Yield: 211.5 mg (0.33 mmol, 66%).

DTA (5 °C min^{-1}) onset: 112 °C (exothermic); IR (ATR, cm^{-1}): $\tilde{\nu}$ = 3153 (w), 3033 (w), 2972 (vw), 2919 (vw), 2891 (vw), 1638 (s), 1623 (s), 1578 (m), 1494 (vs), 1454 (s), 1435 (s), 1393 (m), 1386 (m), 1361 (s), 1349 (s), 1317 (s), 1310 (s), 1298 (m), 1272 (vs), 1231 (m), 1212 (s), 1194 (s), 1175 (s), 1157 (s), 1141 (s), 1090 (m), 1053 (m), 1035 (s), 1017 (m), 1010 (m), 983 (w), 966 (w), 922 (m), 901 (s), 883 (s), 849 (s), 842 (s), 824 (s), 786 (s), 754 (m), 730 (m), 711 (s), 697 (s), 675 (s), 649 (s), 574 (m), 537 (vw), 514 (m), 506 (m), 467 (w), 441 (m), 421 (m); EA ($C_{12}H_{11}CuN_{13}O_{15}$, 640.84): calcd: C 22.49, H 1.73, N 28.41%; found: C 22.31, H 2.02, N 31.87%; BAM drophammer: 4 J; BDIS: > 200 mJ, BAM friction tester: 324 N; ESD: 750 mJ (at grain size ≈ 500–1000 µm).

[Cu(H_2TNPG)$_2$(2-NET)$_4$] (22b)

Complex **22b** was isolated after seven days in the form of green plates blocks suitable for single crystal diffraction experiments. Yield: 524.7 mg (0.43 mmol, 86%).

DTA (5 °C min^{-1}) onset: 105 °C (exothermic); IR (ATR, cm^{-1}): $\tilde{\nu}$ = 3026 (w), 2979 (vw), 2913 (vw), 1652 (vs), 1646 (s), 1627 (s), 1558 (s), 1525 (s), 1520 (s), 1515 (s), 1475 (m), 1460 (m), 1446 (w), 1428 (m), 1405 (w), 1361 (s), 1345 (s), 1305 (m), 1278 (vs), 1216 (s), 1185 (s), 1163 (s), 1145 (s), 1092 (w), 1058 (w), 1043 (m), 1031 (s), 1020 (m), 1007 (m), 963 (vw), 917 (m), 903 (s), 886 (m), 853 (s), 837 (s), 815 (s), 794 (m), 782 (s), 747 (s), 710 (s), 693 (s), 688 (s), 681 (s), 671 (s), 649 (m), 626 (s), 605 (m), 570 (m), 515 (m), 497 (w), 475 (w), 425 (w); EA ($C_{24}H_{24}CuN_{26}O_{30}$, 1220.15): calcd:

C 23.63, H 1.98, N 29.85%; found: C 23.52, H 2.05, N 29.87%; BAM drophammer: 4 J; BDIS: > 200 mJ, BAM friction tester: 324 N; ESD: 750 mJ (at grain size ≈ 500–1000 µm).

$[Cu(H_2TNPG)_2(2\text{-}NET)_4]$ • 2 2-NET (22c)

The co-crystalizing coordination compound **22c** was isolated after ten days in the form of green platelets suitable for single crystal diffraction experiments. Yield: 523.0 mg (0.34 mmol, 68%).

DTA (5 °C min^{-1}) onset: 92 (endothermic), 105 °C (exothermic); IR (ATR, cm^{-1}): $\tilde{\nu}$ = 1651 (s), 1645 (s), 1558 (m), 1513 (vs), 1471 (m), 1457 (m), 1442 (w), 1429 (m), 1360 (s), 1344 (s), 1307 (m), 1279 (vs), 1213 (s), 1192 (s), 1183 (s), 1164 (s), 1146 (s), 1090 (m), 1051 (m), 1037 (m), 1007 (m), 986 (w), 916 (m), 901 (s), 841 (s), 815 (m), 781 (s), 752 (s), 709 (s), 691 (vs), 672 (s), 648 (s), 624 (s), 569 (m), 514 (w), 509 (w), 497 (m), 491 (m), 469 (w), 424 (w); EA ($C_{30}H_{34}CuN_{36}O_{36}$, 1538.36): calcd: C 23.42, H 2.23, N 32.78%; found: C 23.37, H 2.16, N 32.82%; BAM drophammer: 4 J; BDIS: > 200 mJ, BAM friction tester: 60 N; ESD: 750 mJ (at grain size ≈ 100–500 µm).

9. References

S1 CrysAlisPRO (Version 171.33.41), Oxford Diffraction Ltd., 2009.

S2 A. Altomare, G. Cascarano, C. Giacovazzo, and A. Guagliardi, *J. Appl. Crystallogr.*, 1992, **26**, 343.

S3 A. Altomare, G. Cascarano, C. Giacovazzo, A. Guagliardi, A. G. G. Moliterni, M. C. Burla, G. Polidori, M. Camalli and R. Spagna, SIR97, 2003.

S4 A. Altomare, M. C. Burla, M. Camalli, G. L. Cascarano, C. Giacovazzo, A. Guagliardi, A. G. G. Moliterni, G. Polidori and R. Spagna, *J. Appl. Crystallogr.*, 1999, **32**, 115.

S5 G. M. Sheldrick, SHELXL-97, University of Göttingen, Germany, 1997.

S6 G. M. Sheldrick, *Acta Crystallogr. Sect. A*, 2008, **64**, 112.

S7 G. M. Sheldrick, *Acta Cryst. A*, 2015, **71**, 3–8.

S8 A. L. Spek, PLATON, Utrecht University, The Netherlands, 1999.

S9 L.J. Farrugia, *J. Appl. Cryst.*, 2012, **45**, 849.

S10 O. V. Dolomanov, L. J. Bourhis, R. J. Gildea, J. A. K. Howard and H. Puschmann, *J. Appl. Cryst*., 2009, **42**, 339–341.

S11 Empirical absorption correction using spherical harmonics, implemented in SCALE3 ABSPACK scaling algorithm (CrysAlisPro Oxford Diffraction Ltd., Version 171.33.41, 2009).

S12 APEX3, Bruker AXS Inc., Madison, Wisconsin, USA.

S13 M. J. Frisch, G. W. Trucks, H. B. Schlegel, G. E. Scuseria, M. A. Robb, J. R. Cheeseman, G. Scalmani, V.Barone, B. Mennucci, G. A. Petersson, H. Nakatsuji, M. Caricato, X. Li, H.P. Hratchian, A. F. Izmaylov, J. Bloino, G. Zheng, J. L. Sonnenberg, M. Hada, M. Ehara, K. Toyota, R. Fukuda, J. Hasegawa, M. Ishida, T. Nakajima, Y. Honda, O. Kitao, H. Nakai, T. Vreven, J. A. Montgomery, Jr., J. E. Peralta, F. Ogliaro, M. Bearpark, J. J. Heyd, E. Brothers, K. N. Kudin, V. N. Staroverov, R. Kobayashi, J. Normand, K. Raghavachari, A. Rendell, J. C. Burant, S. S. Iyengar, J. Tomasi, M. Cossi, N. Rega, J. M. Millam, M.Klene, J. E. Knox, J. B. Cross, V. Bakken, C. Adamo, J. Jaramillo, R. Gomperts, R. E. Stratmann, O. Yazyev, A. J. Austin, R. Cammi, C. Pomelli, J. W. Ochterski, R. L. Martin, K. Morokuma, V. G. Zakrzewski, G. A. Voth, P. Salvador, J. J. Dannenberg, S. Dapprich, A. D. Daniels, O. Farkas, J.B. Foresman, J. V. Ortiz, J. Cioslowski and D. J. Fox, Gaussian 09 A.02, Gaussian, Inc., Wallingford, CT, USA, 2009.

S14 J. W. Ochterski, G. A. Petersson and J. A. Montgomery Jr., *J. Chem. Phys.*, 1996, **104**, 2598–2619.

S15 J. A. Montgomery Jr., M. J. Frisch, J. W. Ochterski and G. A. Petersson, *J. Chem. Phys.*, 2000, **112**, 6532–6542.

S16 L. A. Curtiss, K. Raghavachari, P. C. Redfern and J. A. Pople, *J. Chem. Phys.*, 1997, **106**, 1063–1079.

S17 E. F. C. Byrd and B. M. Rice, *J. Phys. Chem. A*, 2006, **110**, 1005–1013.

S18 B. M. Rice, S. V. Pai and J. Hare, *Comb. Flame*, 1999, **118**, 445–458.

S19 P. J. Lindstrom and W. G. Mallard, NIST Standard Reference Database Number 69, http://webbook.nist.gov/chemistry/, (accessed March 2021).

S20 M. S. Westwell, M. S. Searle, D. J. Wales and D. H. Williams, *J. Am. Chem. Soc*. 1995, **117**, 5013–5015.

S21 F. Trouton, *Philos. Mag.* 1884, **18**, 54–57.

S22 M. J. Turner, J. J. McKinnon, S. K. Wolff, D. J. Grimwood, P. R. Spackman, D. Jayatilaka and M. A. Spackman, CrystalExplorer17, University of Western Australia, 2017.

S23 NATO standardization agreement (STANAG) on explosives, impact sensitivity tests, no. 4489, 1st ed., Sept. 17, 1999.

S24 WIWEB-Standardarbeitsanweisung 4-5.1.02, Ermittlung der Explosionsgefährlichkeit, hier der Schlagempfindlichkeit mit dem Fallhammer, Nov. 8, 2002.

S25 BAM, http://www.bam.de, (accessed March 2021).

S26 OZM, http://www.ozm.cz, (accessed March 2021).

S27 Military Standard 1751A (MIL-STD-1751A): safety and performance tests for qualification of explosives (high explosives, propellants and pyrotechnics), method 1016, Dec. 11, 2001.

S28 M. S. Gruhne, M. Lommel, M. H. H. Wurzenberger, N. Szimhradt, T. M. Klapötke and J. Stierstorfer, *Propellants Explos. Pyrotech.*, 2020, **45**, 147–153.

S29 NATO standardization agreement (STANAG) on explosive, friction sensitivity tests, no. 4487, 1st ed., Aug. 22, 2002.

S30 WIWEB-Standardarbeitsanweisung 4-5.1.03, Ermittlung der Explosionsgefährlichkeit oder der Reibeempfindlichkeit mit dem Reibeapparat, Nov. 8, 2002.

S31 UN Model Regulation: Recommendations on the Transport of Dangerous Goods – Manual of Tests and Criteria, section 13.4.2.3.3, 2015.

S32 Impact: insensitive > 40 J, less sensitive ≥ 35 J, sensitive ≥ 4 J, very sensitive ≤ 3 J; Friction: insensitive > 360 N, less sensitive = 360 N, sensitive < 360 N and > 80 N, very sensitive ≤ 80 N, extremely sensitive ≤ 10 N. According to the UN Recommendations on the Transport of Dangerous Goods, 5th ed., 2009.

S33 M. Sućeska, EXPLO5 Version 6.05 User's Guide. Zagreb, Croatia: OZM; 2018.

S34 R. Seto, K. Matsumoto and T. Endo, *J. Polym. Sci. Pol. Chem.*, 2014, **52**, 1832–1842.

S35 D. E. Bayes, R. Hayes, P. Blatcher and M. Atkinson, Eu. Pat., 0117368A1, Glaxo Group Ltd., 1982.

S36 W. Finnegan and R. Henry, *J. Org. Chem.*, 1959, **24**, 1565–1567.

S37 M. S. Gruhne, M. H. H. Wurzenberger, M. Lommel, J. Stierstorfer, *Chem. Eur. J.* 2021, in press.

S38 M. H. H. Wurzenberger, N. Szimhardt and J. Stierstorfer, 2018, **140**, 3206–3209.

S39 M. H. H. Wurzenberger, M. Lommel, M. S. Gruhne, N. Szimhardt and J. Stierstorfer, *Angew. Chem. Int. Ed.*, 2020, **59**, 12367–12370.

S40 M. H. H. Wurzenberger, M. S. Gruhne, M. Lommel, V. Braun, N. Szimhardt and J. Stierstorfer, *Inorg. Chem.*, 2020, **59**, 17875–17879.

S41 M. H. H. Wurzenberger, B. R. G. Bissinger, M. Lommel, M. S. Gruhne, N. Szimhradt and J. Stierstorfer, *New J. Chem.*, 2019, **43**, 18193–18202.